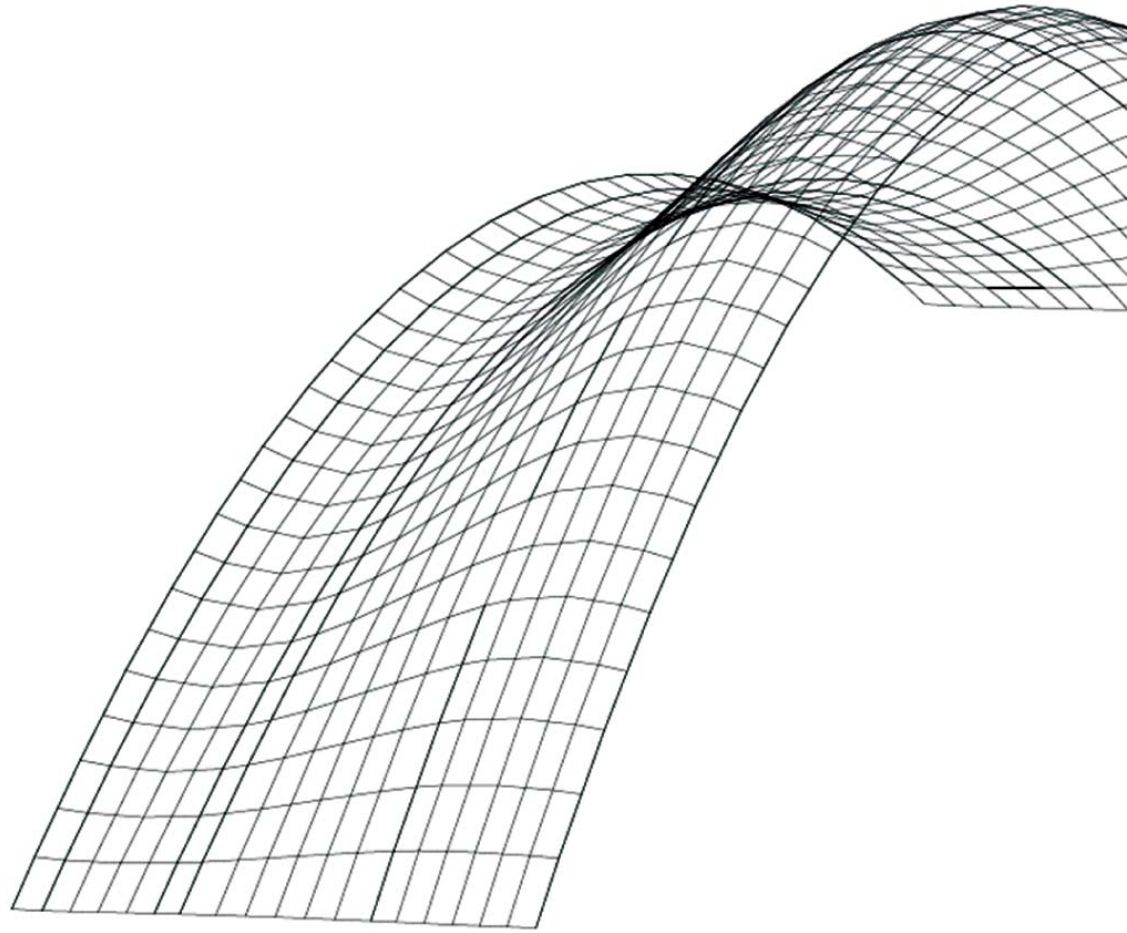




**LUND**  
UNIVERSITY



# **INTEGRATED STRUCTURAL ANALYSIS AND DESIGN USING GRAPHIC STATICS**

ERIK LARSEN

---

Structural  
Mechanics

*Master's Dissertation*

---



DEPARTMENT OF CONSTRUCTION SCIENCES  
DIVISION OF STRUCTURAL MECHANICS

ISRN LUTVDG/TVSM--17/5218--SE (1-66) | ISSN 0281-6679

MASTER'S DISSERTATION

# INTEGRATED STRUCTURAL ANALYSIS AND DESIGN USING GRAPHIC STATICS

Integrerad analys- och strukturdesign  
med grafisk statik

ERIK LARSEN

Supervisors: **VEDAD ALIC**, Licentiate in Engineering, and  
**DANIEL ÅKESSON**, MSc, Division of Structural Mechanics, LTH.

Examiner: Professor **KENT PERSSON**, Division of Structural Mechanics, LTH.

Copyright © 2017 Division of Structural Mechanics,  
Faculty of Engineering LTH, Lund University, Sweden.

Printed by V-husets tryckeri LTH, Lund, Sweden, May 2017 (PI).

**For information, address:**  
Division of Structural Mechanics,  
Faculty of Engineering LTH, Lund University, Box 118, SE-221 00 Lund, Sweden.  
Homepage: [www.byggmek.lth.se](http://www.byggmek.lth.se)



“

*Through history, development of new materials has inspired engineers and architects to create new structures and new architecture. Structural performance and economy were leading design factors that in many cases led to elegant, material effective solutions. In the new architecture, the external shape is usually the priority. Material efficiency and structural solutions are only second. In this perspective, not all new architecture is aligned with the sustainability goal. If cooperation between architects and engineers in early stages of design is adopted, new architecture in line with the demands of this time is possible.*

”

*Sture Samuelsson, Ingenjörens konst (2014)*

*[Translation by thesis author]*



## ABSTRACT

Numerical methods are the norm in modern structural engineering practice. Models based on elasticity theory offer powerful methods to analyse complex structural behaviours and accurately predict probable deformation behaviour. Numerical methods in general and particularly finite element methods offer great numerical accuracy. Yet the tendency is that with increased accuracy come the downside of decreased design capabilities. This is reflected in construction industry practice, where analysis by convention follows design in a largely linear process.

Sketching and model interaction sometimes provide more insight and inspiration than complex models. Graphic statics naturally provides for a sketch-like analysis workflow. Graphic statics is a sandbox term including a variety of graphical structural analysis and design methods useful for understanding and exploring structures. The benefit of such a tool is potentially contribution to; *material sustainability, architectural developments based in honest design and reduced projection costs.*

A simple suspension system, a barrel vault and a Gaussian vault are designed and analysed using traditional graphic statics methods. The effect of structural form on structural efficiency is illustrated and graphic statics form finding capabilities are explored.

Computational graphic statics is explored from two perspectives; how it may be implemented and its application potential. A strategy for computer implementing graphic statics is presented. The algebraic graphic statics strategy successfully representing graphs and the reciprocal relationship but feature some limiting complexities concerning user control. The main benefit and potential of software implemented graphic statics is the option to extend the inherent form finding capabilities and integration with optimisation strategies.

It is finally concluded that besides some niche applications in practice, the greatest benefit of graphic statics is as an educational tool teaching model consideration and structural exploration.



## **ACKNOWLEDGMENTS**

This thesis was authored in 2017 as a final part of the M.Sc Structural engineering program at Lund University, Institute of Technology.

This thesis topic is heavily influenced by the work of Sture Samuelsson, William F. Baker, Caitlin Mueller, Philippe Block, Eladio Dieste, Edward Allen and Waclaw Zalewski amongst others; by who the ideals of form and force in this thesis are inspired. I am personally grateful to them for inspiring this project in which I have had excellent opportunity to study their work and the wide extents of structural engineering.

I would like to thank my thesis supervisors; Vedad Alic and Daniel Åkesson for invaluable guidance. Especially for their support in moments of doubt and for allowing the thesis to take me on an explorative path. I also want to thank thesis examiner Prof. Kent Persson for showing patience, support and humour. It has been a pleasure working with and learning from you!

I extend my gratitude to friends, family and colleagues; without whom I would have lost my sanity because of this project.

MALMÖ, MAY 2017



# CONTENTS

<b>Problem statement</b> .....	<b>XI</b>
<b>Thesis aim</b> .....	<b>XI</b>
<b>Thesis objective</b> .....	<b>XI</b>
<b>Thesis outline</b> .....	<b>XI</b>
<b>Thesis limitation</b> .....	<b>XI</b>
<b>Part I. Traditional Graphic statics</b> .....	<b>1</b>
1.1 Introduction .....	2
1.2 Suspension bridge .....	4
1.2.1 Set up .....	5
1.2.2 Structural exploration.....	6
1.2.3 Concluding remarks.....	9
1.3 Barrel vault .....	10
1.3.1 Model .....	10
1.3.2 Set up.....	11
1.3.3 Alternative funicular structures.....	13
1.3.4 Semi-circle analysis.....	18
1.3.5 Discussion.....	20
1.3.6 Proposed structural system .....	21
1.4 Gaussian vault.....	22
1.4.1 Model .....	23
1.4.2 Method.....	23
1.4.3 Case introduction.....	26
1.4.4 Design process.....	27
1.4.5 Results .....	28
1.4.6 Discussion of model.....	30
1.4.7 Discussion of results.....	31

<b>Part II. Future Graphic statics .....</b>	<b>33</b>
2.1 Introduction .....	35
2.2 Structural optimization using graphic statics .....	35
2.3 Evolutionary design space exploration .....	40
2.4 Discussion.....	43
<b>Part III. Computational Graphic statics.....</b>	<b>45</b>
3.1 Introduction .....	47
3.2 Definitions.....	47
3.3 Algebraic graph representation .....	48
3.4 Reciprocity and equilibrium conditions .....	49
3.5 System self-stress and independent edges.....	51
3.6 Structural exploration .....	52
3.7 Discussion.....	54
3.8 User interface.....	54
3.9 Proof of concept.....	55
3.2 Discussion.....	59
<b>Conclusion.....</b>	<b>61</b>
<b>References .....</b>	<b>63</b>

## **PROBLEM STATEMENT**

*To successfully leverage structural analytics as a source of creativity in architecture design practice; analytical tools that encourage structural exploration need to be developed and their potential recognised by engineers and architects alike.*

## **THESIS AIMS**

To contribute to increased awareness of structural engineering potential as inspiration of good architecture; considering values of sustainability, design honesty and economy.

## **THESIS OBJECTIVES**

To present traditional graphic statics methods, future graphic statics methods and a strategy for computer implementation of the Graphic statics model.

To illustrate the structural exploration capabilities of traditional graphic statics and the potential capabilities of future graphic statics. As such, illustrate the potential of graphic statics to enhance the form finding process.

## **THESIS OUTLINE**

This thesis is divided into three parts where focus is on the first.

The first part will introduce the graphic statics model and present the application of the traditional methods to a variety of structural systems. Three case studies of different structures typologies are presented. The case studies highlight the application of graphic statics at increasing levels of structural complexity and the structural exploration capabilities of traditional graphic statics.

The second part serves to introduce a computational graphic statics strategy. A strategy for automatic reciprocal transformation between form and force graphs is presented and a proposed user interface implementation is presented as proof of concept. The purpose of this part is to form a basis of understanding of future graphic statics software methods.

The third part is a literature review of pioneering developments and research intentions concerning graphic statics. The reviewed examples highlight the benefits of graphic statics model in structural exploration and optimisation software tools.

## **THESIS LIMITATION**

The focus of this thesis is graphic statics methods related to funicular structures and structures that may be analysed in analogy with funicular structures.



**PART I**  
TRADITIONAL GRAPHIC STATICS



## 1.1 Introduction

Initially developed in the late 19<sup>th</sup> century and forgotten in the age of computers, graphic statics has made a recent comeback in pioneering structural engineering research and practice. The advantage of graphic statics is its interactive format and unification of form and forces.

Graphic statics is as the name appropriately suggests a graphical approach to studying statics of structures. While numerical methods are essential for complex structural analysis; sketching and model interaction sometimes provide more insight and inspiration. Graphic statics can be used as a method of structural analysis that encourages sketching. Graphic statics is a sandbox term including a variety of structural analysis methods useful for understanding and exploring structures.

Graphic statics is applicable to any structure that may be considered in analogy with systems of straight members connected in nodes. Although only a few types of structures may be accurately modelled as a system of axial members, many others may potentially be analysed for structural safety using the simple model analogy.

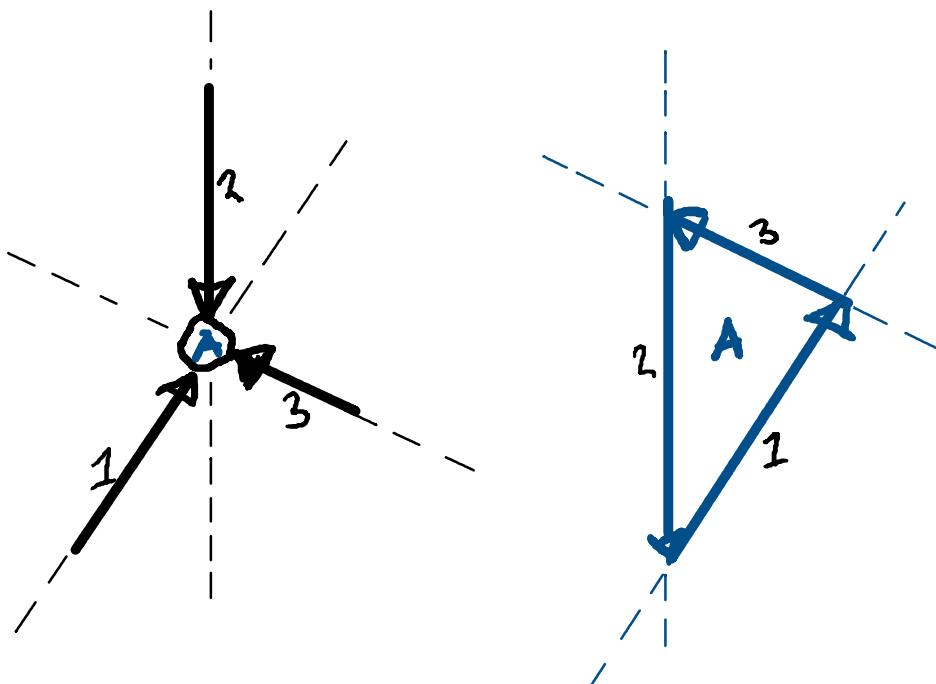


Figure 1. Reciprocal equilibrium systems.

Graphic statics utilises two graphs in parallel. One graph representing the structural form and the application of external forces and the other representing the equilibrium of internal and external forces in the structure. These graphs are referred to as *Form-* and *Force-* graphs.

Form and force graphs are reciprocal. Figure 1 above illustrates this basic relationship. Graphs are said to be *duals* when the nodes in the first graph refer to the surfaces of the second the same way as the nodes of the second refer to the surfaces of the first. Since edge 1, 2 and 3 intersect node 'A'

and enclose surface 'A', the left and right graphs are duals. Since edges are also parallel, the graphs are also *reciprocal*. Reciprocity is the key concept of graphic statics.

Equilibrium is understood in analogy with the graphic vector addition method. Any point in space may be analysed for force resultant as the vector sum of all forces intersecting that point. The resultant force in node 'A' in figure 1 is the vector resultant of force 1, 2 and 3. If node 'A' is in equilibrium the vectors form a closed polygon enclosing a surface we refer to as 'A'.

When a structure grows beyond the complexity of an independent node the graphic statics labelling convention called *Bow's notation* is employed to organise the form and force graphs. The labelling convention guides the reciprocal relationship and is essential to any graphic statics methods. It is by applying and using Bow's notation that one can transform the form graph to the force graph and vice versa.

**1.2 Suspension bridge**

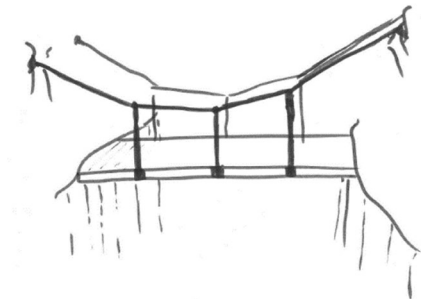


Figure 2. Illustration of modelled suspension bridge.

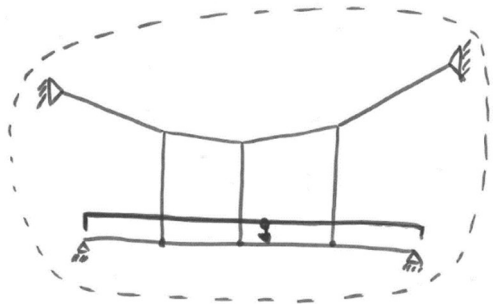


Figure 3. Statics model

A simple suspension bridge illustrated in figure 2 should be modelled and analysed using graphic statics. The forces 'F' in each vertical cable may be estimated to 13kN from static model (figure 3). The forces are shown in figure 4. The suspension system can be studied by use of graphic statics. The suspension system is accurately comparable to a network of axial members intersecting in nodes.

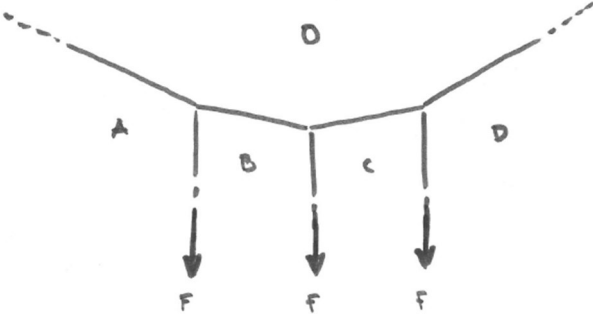


Figure 4. Form graph representation

### 1.2.1 Set up

This section will review how the form and force graphs are set up by employing Bow's notation.

Bow's notation convention is a method to organise the reciprocal transformation between the form and the force graph. It is also helpful to interpret the graphs. Considering reciprocity, surfaces in the form graph are reciprocal to nodes in the force graph. As such, the labelling follows that the form graph surface labelled 'A' will be the reciprocal to force graph node labelled 'a'.

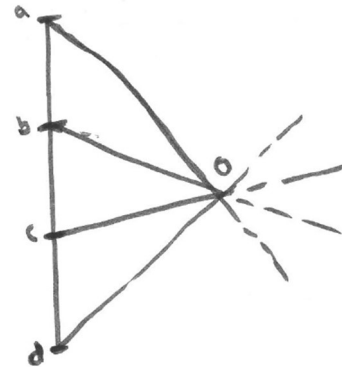


Figure 5. Force graph

The form graph edges in figure 4 divide the graph into surfaces. In this case, no surface is fully enclosed by edges, and as such these are referred to as *external* surfaces. Surfaces fully enclosed by edges, such as the internal parts of a truss form graph, are referred to as *internal* surfaces. The difference is mainly one of terminology when applying labels to surfaces using Bow's convention; external surfaces are labelled first followed by internal surfaces. Form graph surfaces are by convention labelled using capital letters and sometimes numbers for internal surfaces.

Corresponding edges in form and force graph are parallel. In this case, form graph edge A-B will be parallel to force graph edge a-b. With bows notation dictating the reciprocal relationship between the graphs it is possible to transfer edges from form graph to force graph and thus finding the magnitude of all forces.

The construction of the force graph shown in figure 5 starts by the drawing a force line. The force line is constructed of all external forces applied to the structure. The labels in the force graph correspond to the labels given to surfaces in the form graph. For each force line, the head and tail node is given the labels of adjacent surfaces to corresponding form line. The force line is labelled at its tail by the form surface label to its left and at its head by the form surface at its right.

External force 'A-B' is transferred to the force graph and will form the beginning of the force line. Node 'a' can be determined arbitrarily. As the force is vertical in the form graph so is the edge connecting node 'a' and 'b'. The length of 'a-b' represents the force magnitude. As the force magnitude is determined as 13kN the force edge length should represent 13kN, thus defining the position of node 'b'. External force 'B-C' is transferred to force graph to form edge 'b-c'. The direction and the magnitude is transferred and since 'b' is already defined, node 'c' is consequently defined.

The magnitudes of internal forces 'a-o', 'b-o', 'c-o' and 'd-o' is initially unknown. The magnitudes are found by connecting respective edges to defined nodes 'a', 'b', 'c' and 'd'. Point 'o' is found as the intersection of the edges adjacent to form surface 'O'.

### 1.2.2 Structural exploration

Two different structural variations will be explored for function and performance. First, different fastening locations against the rock wall will be explored for efficiency. Second, slack on the primary cables will be explored for efficiency.

A simple evaluation criterion is useful to evaluate material efficiency considering a static load. The total *system force length* may be estimated and used for criteria. With member length 'L' gathered from graph and internal member forces 'P' gathered from force graph the evaluation criteria may be expressed by equation 1 (Beghini, 2014). An approximate average stress may be assumed. The total force length divided by the assumed stress gives an approximate total structural volume.

$$(1) \quad \sum_{i=1}^n P_i L_i$$

Three different fastening positions will be considered. The right side fastening position; an elevated position, a medium and a low. The challenge is to find a funicular suspension line for each position. With the force line determined, funicular variations can be explored as a function of origo position in the force graph. How to proceed is a matter of personal preference.

With the fastening positions and the force line given, a funicular may be constructed by simply selecting an arbitrary force graph origo 'o'. Given 'o', edges 'a-o', 'b-o', 'c-o' and 'd-o' may be transferred to the form graph using bows notation.

One way of finding a suitable 'o' considering the design space is to have form edges 'A-O' and 'D-O' intersect at desirable approximate lower limit of the funicular suspension line. Here, 'A-O' and 'D-O' are taken to intersect the lower edge boundary between spaces 'B' and 'C'. The resulting funiculars are illustrated in figure 6 (left) single, double and triple dash-dot lines marking the elevated, the medium and the lower funicular respectively.

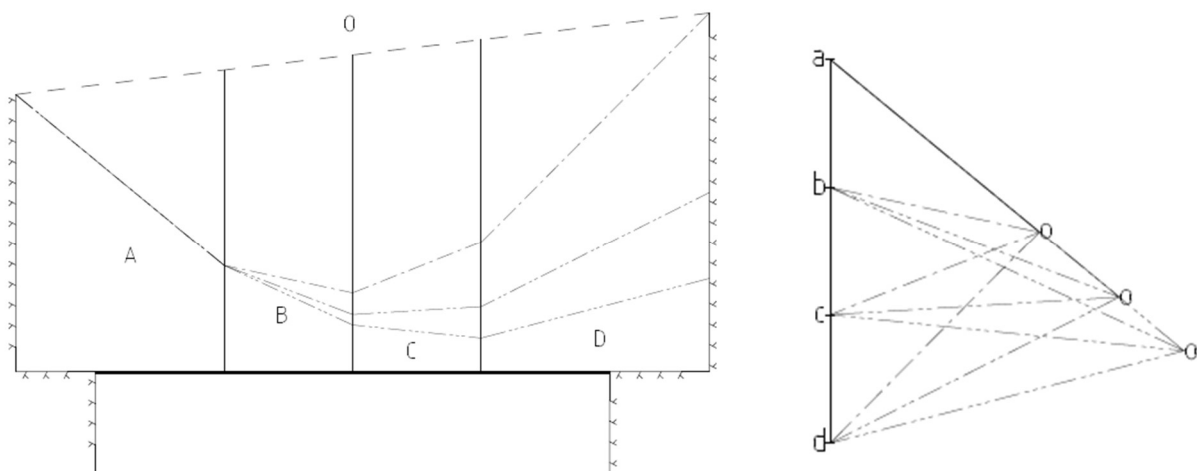


Figure 6. Form graph (left) and force graph (right). Single-, double- and triple- dash-dot line representing funicular variations.

The slack variation may be explored using the same method. Here four different slack depths are considered. With fastening positions and force line determined, designer preferences may guide funicular properties.

Here, edges 'A-O' and 'D-O' are again taken to intersect at the lower edge boundary between surfaces 'B' and 'C' from which the position of 'o' is determined and the funicular is constructed. Resulting funiculars are illustrated in figure 7.

Internal forces and member lengths are simply measured in the force and form graphs respectively. The results are presented in table 1 below.

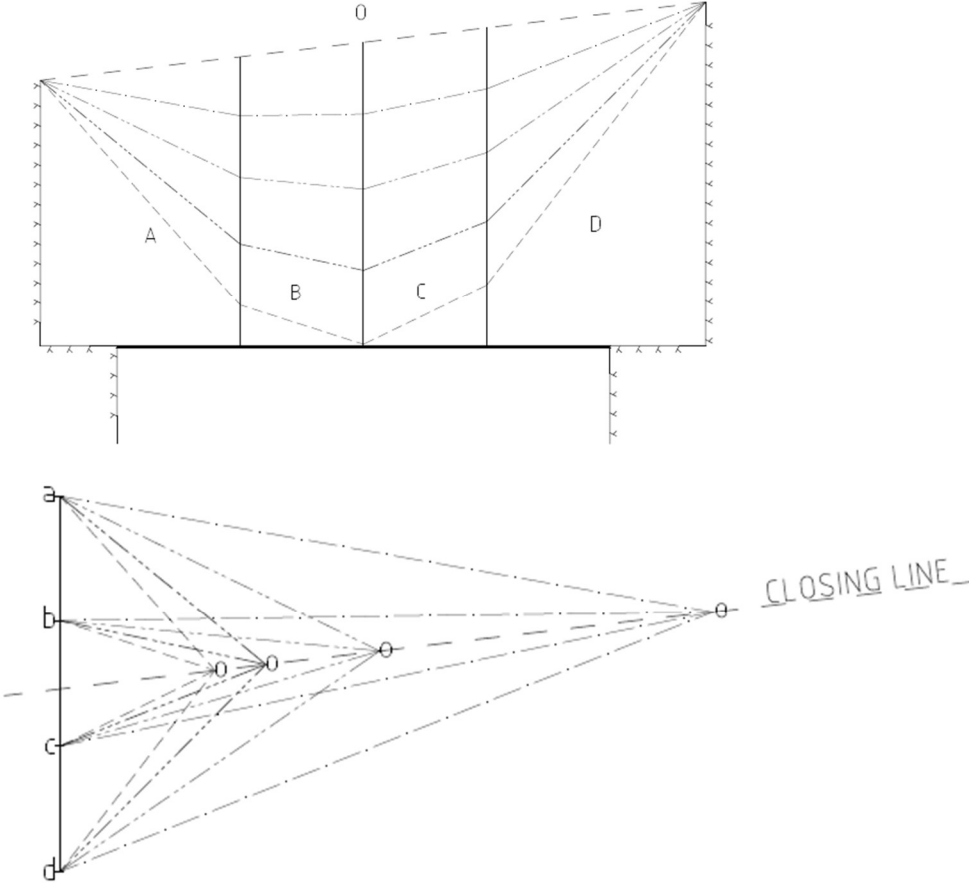


Figure 7. Form graph (top) and force graph (bottom). Single-, double- and triple- dash-dot and dashed lines representing funiculars variations.

Edge	<u>Slack variation</u>				<u>Fastening position</u>			
	Most shallow	Less shallow	Less deep	Most deep	High	Medium	Low	
<i>a-o</i>	69	37	28	24	28	38	47	[kN]
<i>b-o</i>	68	33	22	17	22	31	40	
<i>c-o</i>	69	35	23	18	23	29	36	
<i>d-o</i>	73	40	30	26	30	33	37	
<i>A-O</i>	6,2	6,8	7,9	9,2	7,9	7,9	7,9	[m]
<i>B-O</i>	3,8	3,8	3,8	3,9	3,8	4,0	4,1	
<i>C-O</i>	3,8	3,9	4,0	4,2	4,0	3,8	3,8	
<i>D-O</i>	7,2	8,1	9,4	10,9	9,4	7,4	6,9	
$\sum_{i=1}^n P_i L_i$	1473	837	680	651	680	782	923	[kNm]
% of best	226%	129%	105%	100%	105%	115%	136%	

Table 1. Internal forces, edge lengths and resulting total force length of respective funicular variation.

The *total force length* criteria indicate that total required structural volume significantly decrease with funicular depth.

As one may intuitively expect shallow funiculars result in larger internal stress than deep funiculars. Force graph results suggest an *exponential* increase of stress for corresponding linear decrease of funicular depth. Notably, after a certain depth the further decrease of stress compared to further increase in depth of the arch is marginal.

### 1.2.3 Concluding remarks

The example illustrates the fact that structural form greatly influences structural performance. As illustrated, even variations on the same topology result in significant differences in internal forces. This study excludes alternative topologies and alternative structural systems for which even greater performance may be possible.

The significance of structural performance may not be a virtue on its own but rather it as an important means to an end. Considering the correlation between internal forces, member sizes and function, it is significant as a means to *align vision with end result*.

If the structural form is not designed in line with structural performance it may result in awkward member sizes, uneconomical demand for high performance materials and affect the longevity of the structure (Beghini, 2014)

The simplistic Graphic statics model also serves as a reminder of structural honesty. The notion of structural honesty is one where observers are assumed to have an

intuitive sense of the properties of materials. Honest design considers it important to utilise materials in line with their characteristic properties. Structural honesty encourages the structural form to be developed in line with the properties of selected materials as to achieve harmony between form and forces. Materials not used in line with properties are considered decorative and to 'cheat' the observer. As no material prefers bending to axial forces, graphic statics naturally encourages designs aligned with structural honesty.

Utilising materials in line with their properties is also a key to achieving some spectacular designs. High performance structures have throughout history pushed the boundaries of what is possible with available materials. Either to achieve long spans, extreme height or expressive form; to push the limits of materials it is necessary to develop the structural form in line with the properties of selected materials. Exhibiting an elegance expressive funicular form, the Schwandbachbruecke (Picture 1) is one such structure testifying of the capacity of honest design.



Picture 1. Schwandbach bridge by Robert Maillart 1933. (Source: Xpowa - Own work, CC BY-SA 3.0)

### 1.3 Barrell vault

Nyhamnen is a part of the old industrial harbour in Malmö, Sweden. The area is under transformation to a modern mixed-use area. A design challenge was set up to gather conceptual designs of potential landmark buildings for the area.

Architect Karolina Pajnowska envisioned a building that is ‘*anonymous and timeless* in its mainframe’ such that different cultures would relate differently and therefore create new use for the building during its lifespan. Drawing on the value of timelessness, the building is intended to *stand the test of time* (Pajnowska, 2016).

The study presented by the architect was intended as a vision and program of the building function. To develop the vision into a design, engineers were invited to collaborate in preliminary studies.

The initial structural design vision includes several expressive structural barrel vaults and a large roof dome. To *stand the test of time*, the structural geometry and the correct utilization of the properties of bricks are essential. Graphic statics is an excellent tool to analyse structural behaviour of brick vaults. Such a process will be demonstrated in this case study.

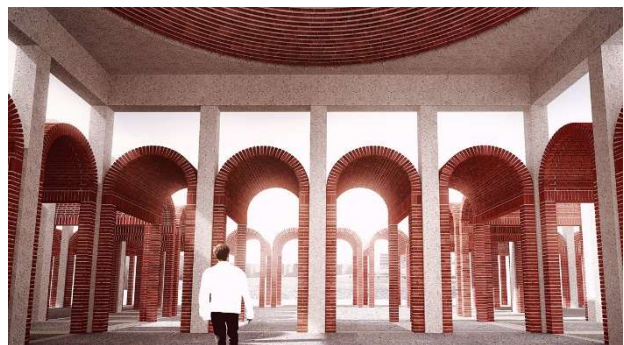
The example will illustrate two graphic statics methods. Alternative ideal arch geometries will be explored first. After that, the proposed semi-circle arch geometry will be analysed. It will be analysed for equilibrium and crack propagation.

#### 1.3.1 Model

Although visually simple to comprehend arches are indeterminate (Heyman, 1995) and complex to analyse. Originally, geometric rules discovered by trial and error guided the design of arches (Block, 2005). In 1675 Robert Hooke discovered that arches may be analysed in analogy with hanging flexible lines. This analogy aided the design of rigid arches beyond the constraints of trial and error. Hooke elegantly expressed his discovery as:

*As hangs the flexible line, so but inverted will stand the rigid arch* – Robert Hooke 1675.

A flexible line will adapt its shape under a static set of loads. If the load distribution changes, so does the form of the flexible line. This force adapted form is referred to as funicular tensile line. What Hooke states is that for any rigid standing arch, a funicular *thrust* line may be identified within its boundaries.



Picture 2, renderings of Nyhamnen project. Studied vaults shown. (Source: Karolina Pajnowska)

Hooke's statement does not predict the true mechanics of a rigid arch. The true working mechanics are due to its width, imperfect geometry and inhomogeneous material highly indeterminate, thus unpredictable.

To analyse a proposed arched design with Hooke's analogy one may imagine a flexible line fixed between the arch supports and exposed to the arch set of static loads. The line will deflect to a funicular tensile form. If a funicular shape may be found that [mirrored] fit within the boundaries of the proposed arch design, one way of equilibrium is possible.

If a single thrust line may be found within the boundaries of the arch a theoretical equilibrium between static loads and support reactions is possible (Block, 2006). When designed with sufficient capacity for internal forces in theoretical equilibrium, the arch may be considered rigid.

The designed funicular thrust line does not represent the actual state of the built arch but it does provide a possible equilibrium state.

### 1.3.2 Set up

Utilising Hooke's thrust line analogy we construct an initial form graph by roughly tracing the centre line of the vault illustrated in fig. 8. The arch is divided into ten pieces of equal horizontal length. This geometry is primarily used to create an initial force distribution.

Using this preliminary form, we may calculate and apply the external forces. The external forces are calculated from a uniform (presumed) dominant load case and the tributary area of each node, resulting in the force line fig. 9.

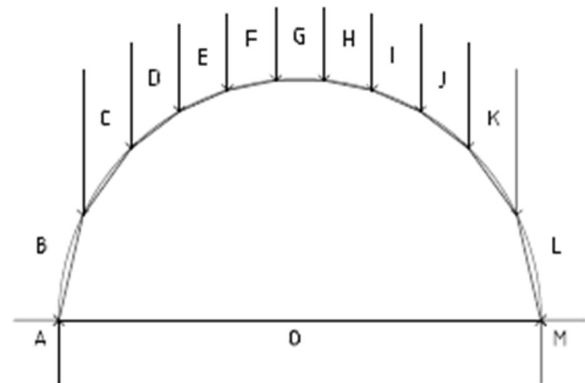


Figure 8. Initial approximate model

It may be noted that initial form is not in equilibrium with external forces. As all internal edges of the form graph face surface 'O', all edges in force graph except force line should intersect in 'o' for equilibrium.

Due to the non-funicular geometry significant horizontal forces need to be included in order to achieve equilibrium in the form. The resultant increase in magnitude, from small at the crown to large at nodes closest to supports.

The additional horizontal forces may be visualised by studying individual force polygons. Fig. 10 show individual vectors sums belonging node B-C-O, C-D-O, D-E-O and E-F-O. The distance between the 'O's in each polygon is resultant force addition to the horizontal thrust developed in that segment.

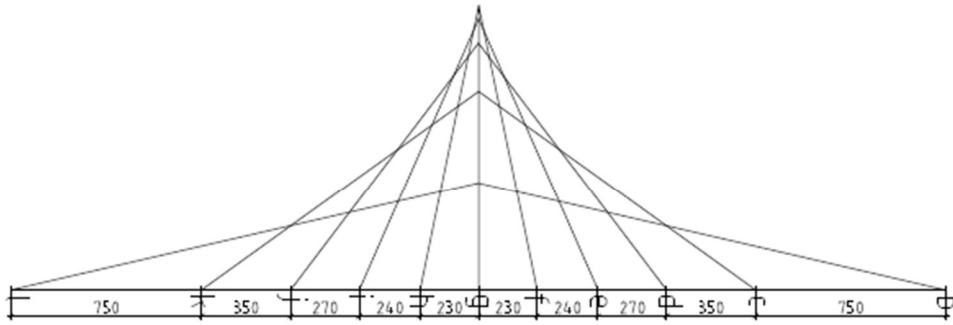


Figure 9. Incomplete force graph of approximate form and load case. Graph does not comply with Bows notation.

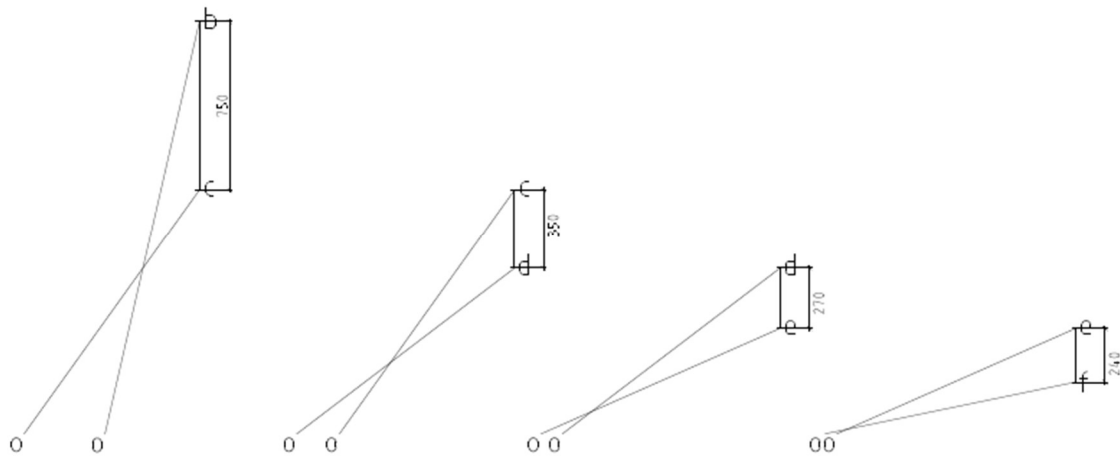


Figure 10. Individual polygons B-C-O, C-D-O, D-E-O and E-F-O

### 1.3.3 Alternative funicular structures

One strategy to achieve equilibrium is to modify the form. In this section three structural variations will be pursued; one where the thrust line is tangent top of semi-circle arch (fig 11, left), one where the angle of the lower parts of funicular tangent semi-circle angle close to support (fig 11, middle) and one that is a compromise between the two previous (figure 11, right). Exploration is limited to three alternatives for demonstration purposes. Of course, design variations are only limited by imagination and the proposed designs should inspire further collaborative explorations.

The graphic statics pioneer William S. Wolfe laid out a general method to generate a funicular arch. His method is general in the sense that it works for any uniform or non-uniform load case (Wolfe, 1921). The generated funicular will pass through three assigned points with a geometry adapted to the specified load case. Table 2 describes and illustrates this method as applied to the case vault studied in later section of this thesis.

Under certain circumstances a simplified method may be applied as described by Edward Allen and Waclaw Zalewski in *Form and forces* (2010). For this method to be applicable it is necessary that the loads are equally distributed along the horizontal component of the structure and the span to rise ration needs to be greater than or equal to 4:1. For any ratio less than 4:1 the method may still be applied under careful consideration of necessary degree of accuracy.

An infinite number of funicular alternatives may be identified per load case using Wolf's method. As stage 1 and 2 described below are related to the force graph, once 'U' and 'V' are located, their position may be reused to generate any number of form alternatives to the same load line. Alternatives are easily explored by repeating stage 3 and 4. Form constraints may be incorporated by experimenting with stage 3 and 4.

Here, Wolf's method requires three points to be prescribed, and which the funicular will intersect. Two points are predetermined as location of supports but third point remain a free variable. This method was used to generate alternative 1 and 3.

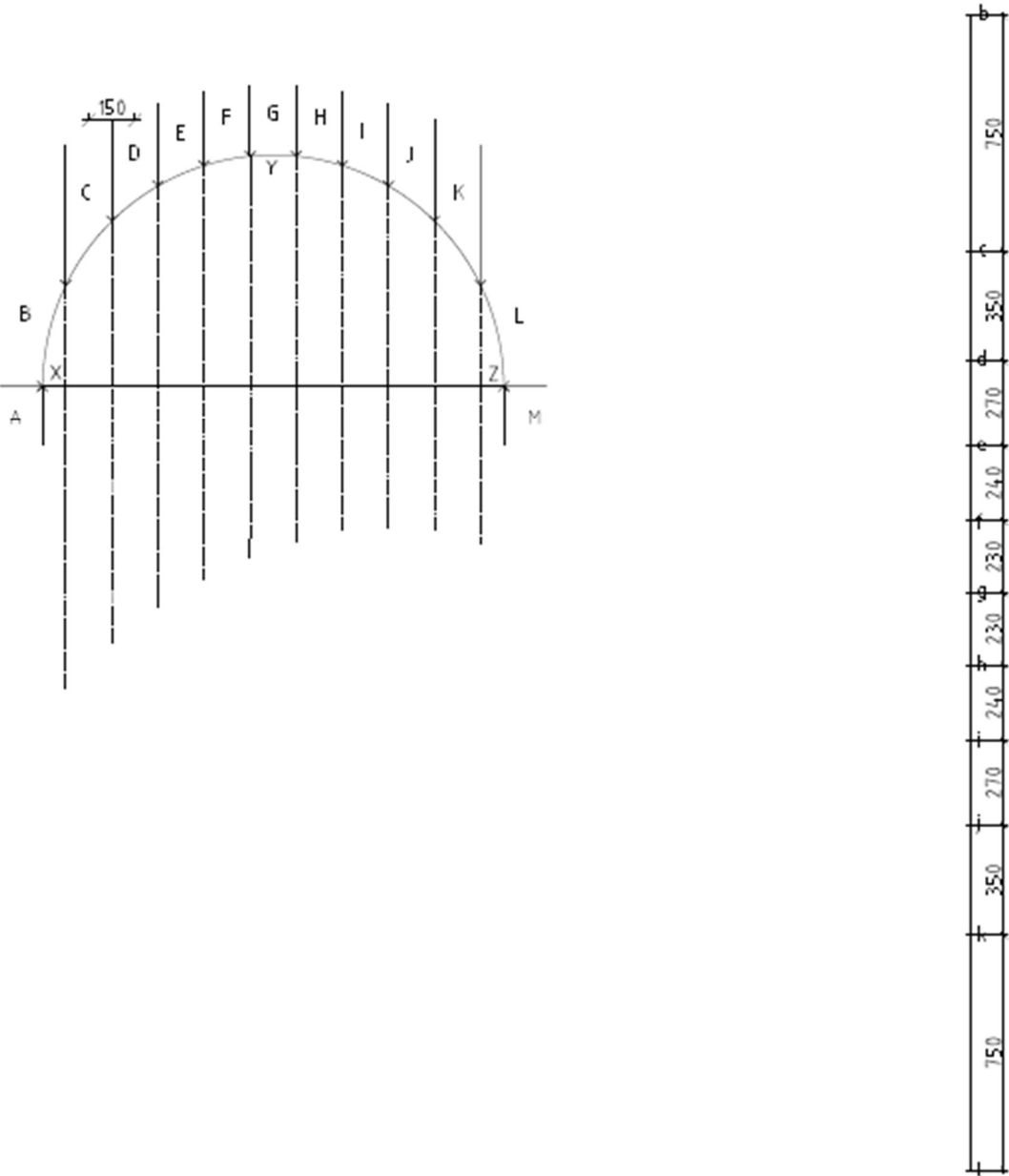
When exploring structural alternatives to the same force line, one should be careful to consider that the force line is applicable in each case. Tributary area will vary a lot depending on the depth of the arch. An initial force line may be used to generate approximate funicular but for improved accuracy one should recalculate the load line as per specific approximate funicular and regenerate funicular.

Figure 11 illustrates design alternatives generated using the methods and incorporating pursued geometric constraints. The funicular intersecting the crown at a tangent is easily achieved by prescribing point 'Y' to that position. The intersection is parallel with initial geometry due to symmetry. The other two alternatives require some iterations. Appropriate angles at support edges are found by testing different positions of 'Y'.

Following steps 1-4 describe the process to develop a funicular geometry for a set of external forces. Two points are decided as fix support points for the funicular line and a third point between the two is decided where the funicular will intersect.

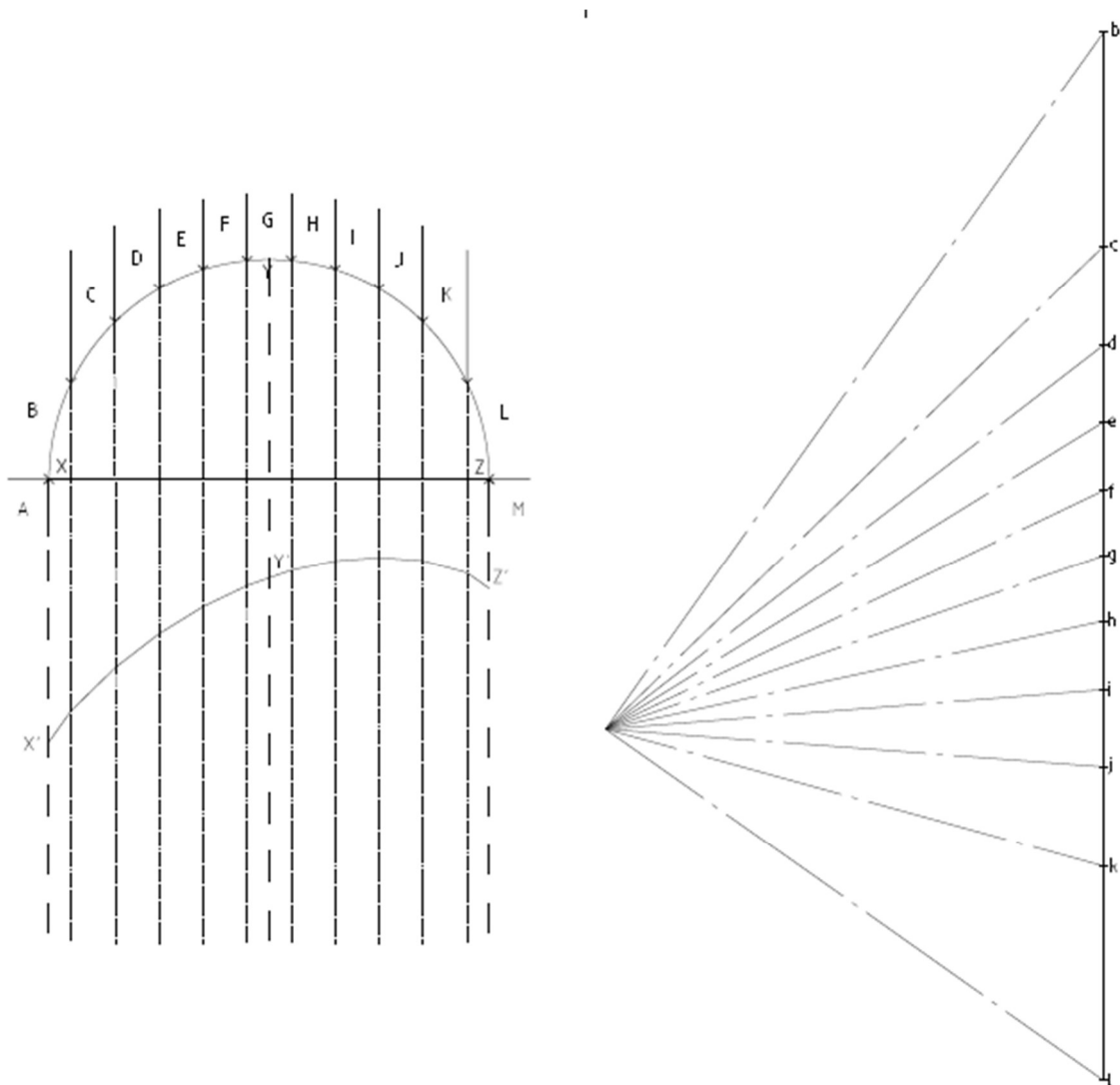
**Step 1:**

- Divide design space into sections and calculate external forces from load case and tributary area.
- Points X, Y and Z mark the three points that the funicular will intersect.



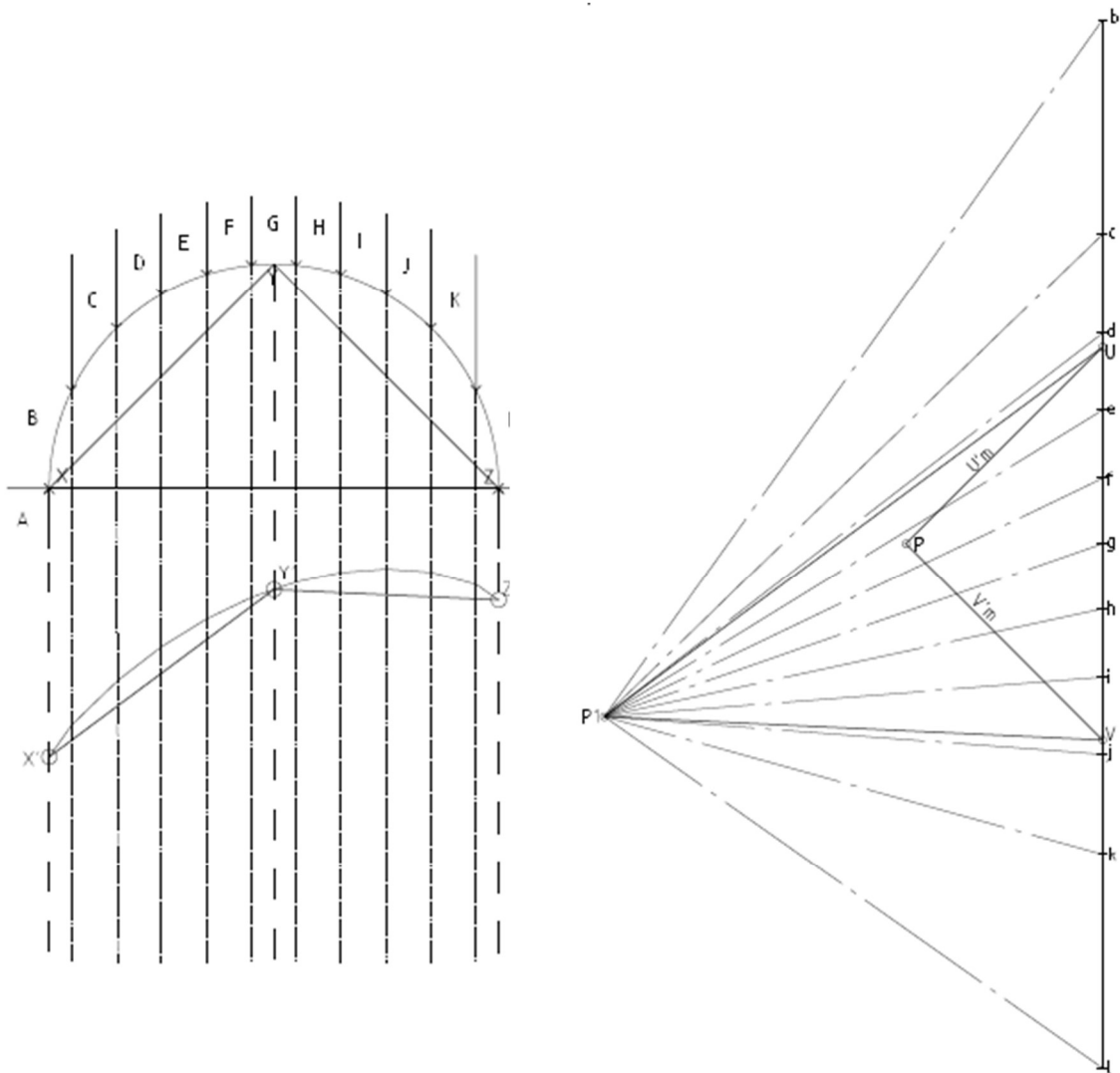
**Step 2:**

- Choose any point  $p_1$  in force diagram.
- From  $X$  and  $Y$  draw lines parallel to the force line resultant  $B-G$ .
- Choose any point  $X'$  along line parallel to force line resultant  $B-G$  originating from  $X$ .
- From  $X'$  construct reciprocal form corresponding to assumed  $p_1$  origo.
- Locate  $Y'$  as intersection of constructed funicular and line parallel to  $B-G$  originating from  $Y$ .
- From  $Z$ , draw a line parallel to force line resultant  $G-L$  and locate  $Z'$  similarly to  $Y'$ .



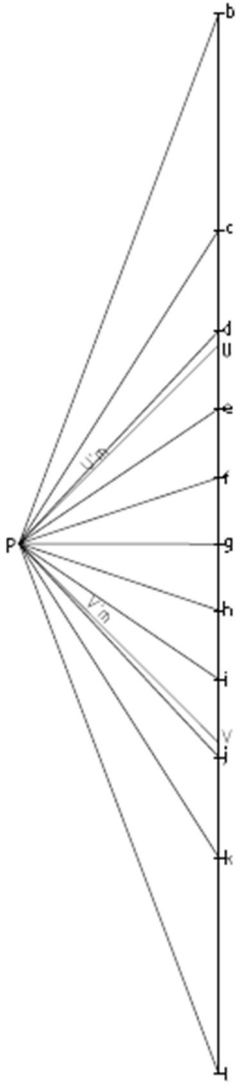
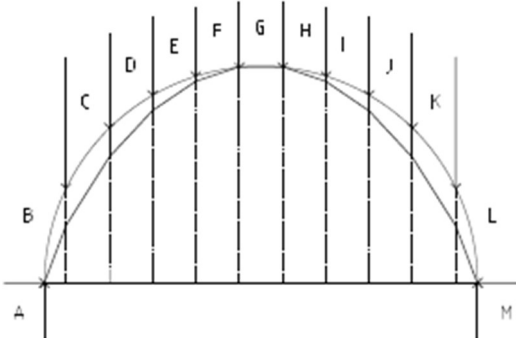
**Step 3:**

- From p1 draw line p1-U parallel to X'-Y' and locate U along force line.
- From U draw the line U'm parallel to X-Y.
- From p1 draw line parallel to Y'-Z' and locate V along force line.
- From V draw the line V'm parallel to Y-Z.
- Intersection U'm and V'm marks the desired origo p.



**Step 4:**

- Construct desired funicular from origo p by transferring edges according to Bow's notation



### 1.3.4 Semi-circle analysis

An ideal arch may be considered structurally safe if a thrust line exist within the boundaries of the structure such that the resultant force at each joint lies within the cone of friction (H. Moseley, 1843). Although the proposed semi-circle geometry obviously is non-funicular it may be rigid in funicular equilibrium. However, conditions are not ideal and Moseley's conditions are not enough in itself to judge structural safety.

The proposed arch is supported on top of relatively slender columns. Although it is likely that a funicular exists within the arch such that Moseley's condition is satisfied, it is equally likely that the horizontal thrust of such a thrust line will cause significant cracking and deflection in columns, thus risking a loss of equilibrium.

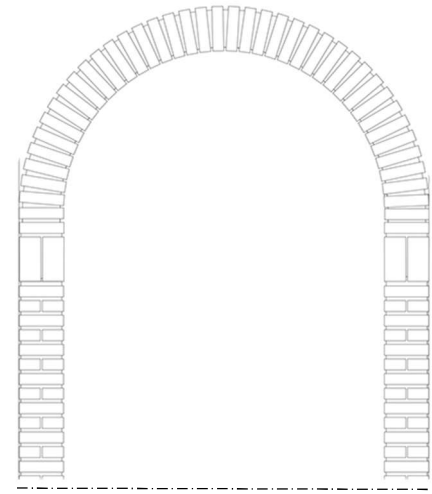


Figure 13, proposed semi-circle vault design.

(Source: Pajnowska, 2016)

An upper bound analytical strategy is to compare the maximum horizontal thrust with column capacity. The horizontal thrust will cause a significant moment at the base of the columns. It is likely that the total limiting factor of the structural system is cracking due to tensile stresses developing at the base of the columns.

The horizontal components of the funicular thrust line will cause a moment in the supporting columns. If the horizontal force is large enough the resulting moment will cause the columns to crack and deflect. The deflection of the columns must be limited in order to limit the crack propagation in the arch. The columns need to be designed with sufficient moment capacity, such that they are able to withstand without crack propagation a horizontal force larger than the horizontal funicular thrust component.

In this case the column design is predetermined and as such also the moment capacity. To analyse the rigidity of the proposed design we may compare the capacity of the columns to withstand a horizontal force, to the maximum horizontal force component that may develop in the proposed arch.

A thrust line with maximum horizontal thrust component is found using Wolfe's method to generate funicular arches. The shallowest funicular is that which touches the lower boundary at the crown of the arch and fits within the outer boundary at the supports. Using the method, point 'Z' is set at the crown lower boundary and support points are iteratively modified until a thrust line is found. The horizontal force component is constant throughout the arch and may be measured as the horizontal distance between the origo and the force line.

The maximum horizontal thrust is 887N/m. This is significant in terms of serviceability and *longevity*. The force is enough to cause a 650kPa tensile stress in the base of the column which is significantly above the typical masonry tensile strength. The upper bound analytical method predicts a significant risk of crack propagation and degradation over time.

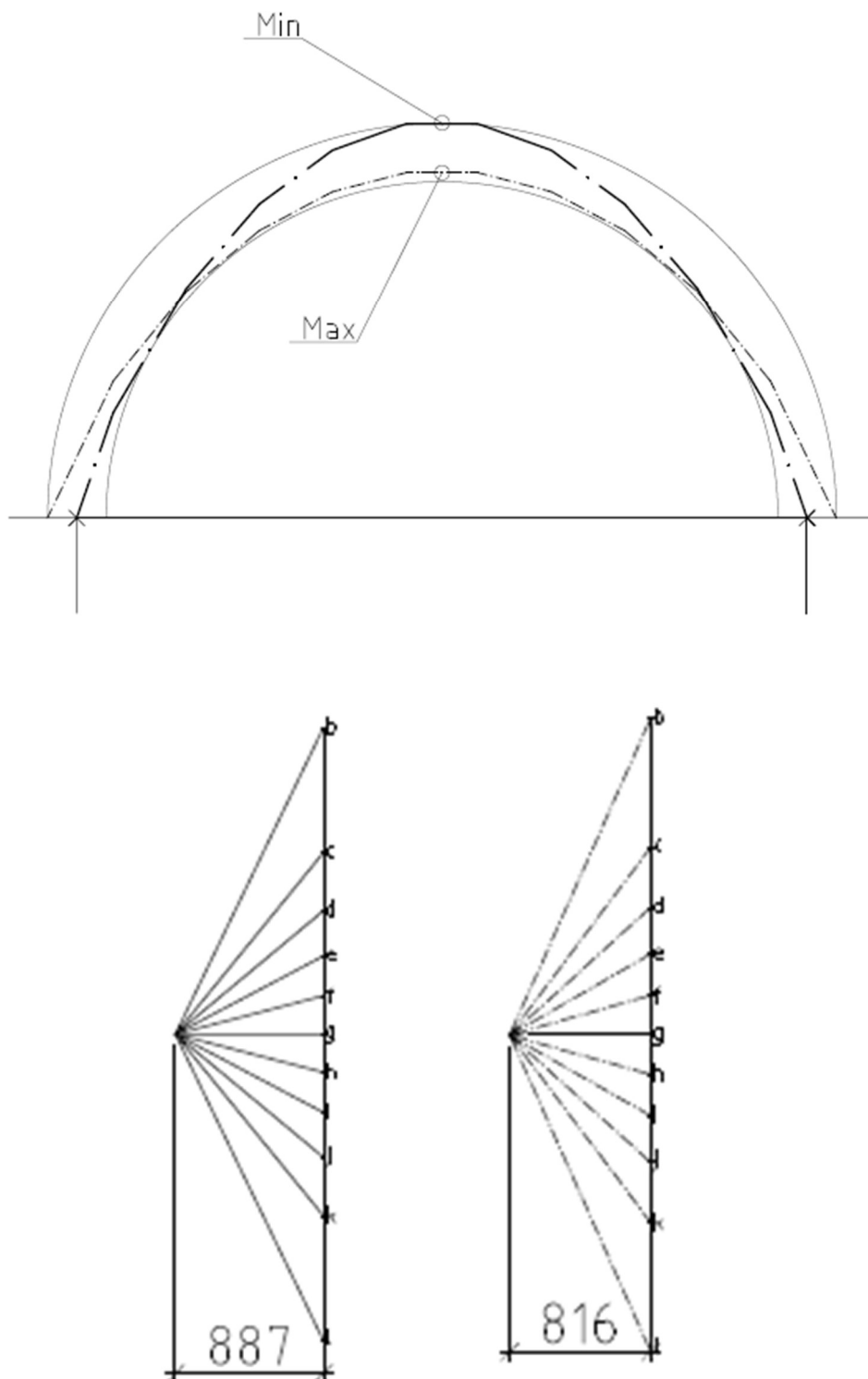


Figure 14. Maximum and minimum thrust lines and corresponding force graphs.

### 1.3.5 Discussion

The presented upper bound analytical method is unlikely to accurately predict the true failure mode. Due to the indeterminate nature of the structure it is impossible to predict the true force path, in fact it is probably not truly funicular.

Even if cracking is initiated by the maximum thrust line, the system may possibly shift to any redundant thrust line that represents an equilibrium state after cracking. As such, it is possible that the structure may remain standing if the columns are capable of resisting the horizontal force exerted by the minimum thrust line. Opposite the maximum thrust line, the minimum thrust line is that which exerts the least horizontal thrust. Using the same procedure as with the maximum, the minimum is found with point 'Y' as close to inner boundary at arch crown.

Due to the minimal thickness of the arch, the minimum horizontal thrust is only marginally lower than the maximum. It is therefore concluded that the proposed structure is likely to develop significant deformations and alternative systems should be pursued in order for structure *to stand the test of time*, as intended.

### 1.3.6 Proposed structural system

The development of cracks in the base of the columns are limiting the structure. It is therefore very beneficial to design the system so that horizontal equilibrium is achieved at the base of the arch without utilising the columns. The left and the right sides of the arch exert similar horizontal thrust. Equilibrium may be achieved by connecting the supports by a simple horizontal cable. This is perhaps the most simple and effective option.

An alternative is to consider the global system with adjacent arches. Assuming equal live-load on each arch and similar active thrust lines, the horizontal force component of respective adjacent arch form a global system horizontal equilibrium. Thus global stability may be achieved by moving arches closer, such that the support each other at the base. This is a common solution found with many systems of arches.

Summarising the findings, an alternative structure is proposed. The proposed structure is conserving initial design intentions but modified to better serve the ideal of *standing the test of time*. As tensile stresses should be avoided in brick work, longevity is best achieved with pure compressive thrust lines. This is achieved by incorporating the funicular arches generated previously and having them touch at the base. The proposed system is arguably an example of honest design. The proposed design should serve as inspiration to further develop the design.

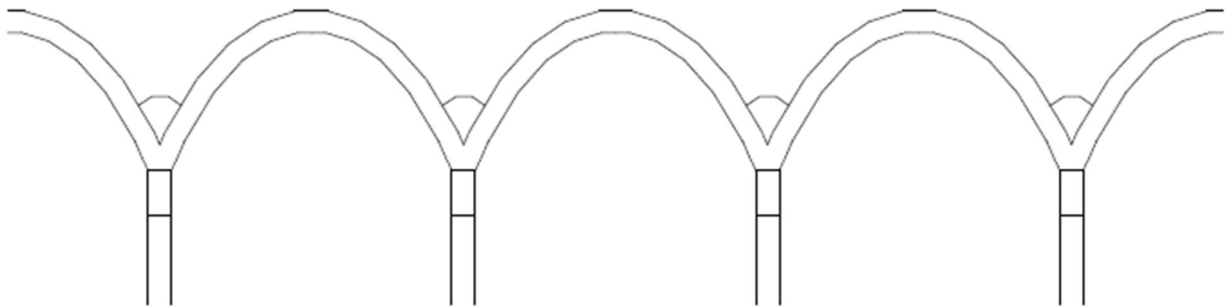


Figure 15. Proposed global system of arches.

## 1.4 Gaussian vault

A Gaussian vault is a type of double curved masonry vault, pioneered by engineer Eladio Dieste. Characteristic of Gaussian vaults are their expressive undulating form and their elegant lightness.

The vault span is large in relation to width, rise and thickness. Dieste's vaults typically have a span to rise ratio between 10:1 and 7:1, with a remarkable thickness of only 130 mm in total!

The construction developed by Dieste consists of a single 100 mm thick layer extruded hollow core clay bricks topped only by a 30 mm thick layer of lightly reinforced cement. Where the primary purpose of the cement was to provide weather tightness. The joints between bricks were filled with a high-grade cement-sand mortar and reinforced in both transverse and longitudinal direction.

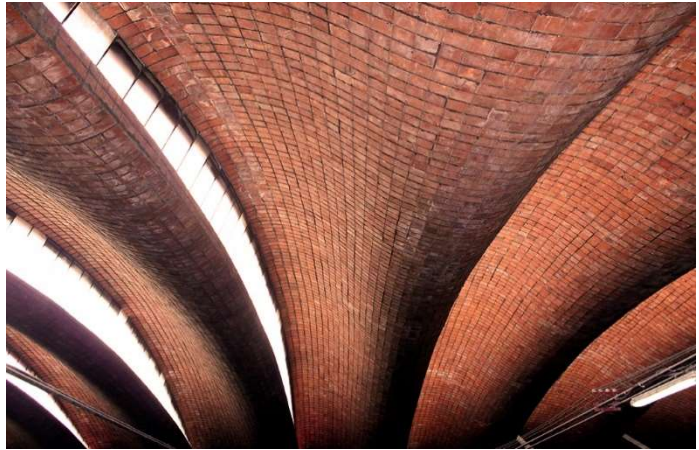
Perhaps equally characteristic of both the vaults he designed and characteristic of his own philosophy of construction is how the

architecture was developed in synergy with the characteristics of the material. It was his belief that 'For architecture to be truly constructed the materials should be used with deep respect for their essence and consequently their possibilities' (Pedreschi and Theodossopoulos, 2007).

Dieste managed to turn traditional brickwork into a material suitable for the modern construction era. Not only was the construction economical and the process rational but the vaults also satisfied requirements for accuracy, efficiency in materials, prefabrication, reliability in performance and analytical rigour (Pedreschi and Theodossopoulos, 2007).

Dieste continuously developed the Gaussian design during his career, gradually perfecting the analysis and construction process. His experience led over time to large projects such as the Growers Pavilion in Brazil (Picture 3) with an impressive span of 47m!

The presented model and method is based on the work of Eladio Dieste as presented by Pedreschi and Theodossopoulos (2007) and Allen and Zalewski (2010). The combined use of graphic and numeric methods will be presented in an illustrative case study format, where a Gaussian vault spanning 30m will be designed. The following section should also dissect and discuss the model assumptions.



Picture 3. Caputto Fruit Plant. Salto Uruguay.

(Original source unknown)

Growers pavilion, Brazil.

(Source: Centrais de abastecimento do rio grande do sul)

### 1.4.1 Model

Although different in its expression, the Gaussian vault behaves structurally very much alike the simple barrel vault studied in the previous section. Every section along the length of the vault is a thrust line in a funicular equilibrium with the supports.

Although the structural behaviour is as simple as funicular thrust lines, the true structural behaviour is indeterminate and thus complex to analyse. It is the intention of this section to illustrate and discuss a simple model and interactive design method that supposedly allows the design of structurally safe Gaussian vaults.

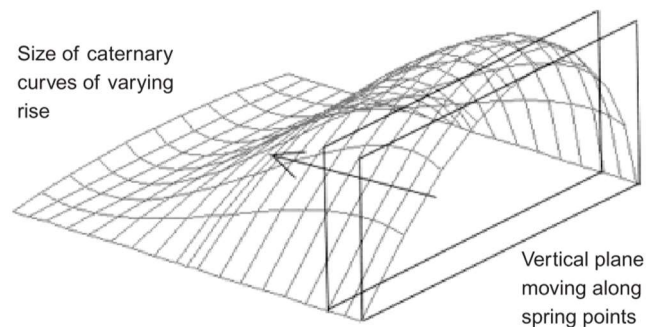


Figure 16. Illustration of a Gaussian vault. (Source: Pedreschi and Theodossopoulos, 2007)

For thin vault structures, the maximum possible span is ordinarily severely limited by buckling. The Gaussian vaults elegantly resist buckling by recruiting the cross-section moment of inertia created by the transverse sections undulation. This is the elegant genius of the Gaussian vaults and the main reason as to why they may span such long distances without awkward bracing systems reducing the elegance of the system.

Designing the undulation against buckling is the main analytical challenge but one that Dieste managed to solve. His numeric formulas provide a uniformly distributed load under which the system would buckle. This approach is analysed and compared with a FE Analysis by Pedreschi and Theodossopoulos (2007) to satisfactory results.

### 1.4.1 Method

Three design cases are dominant and need to be considered for the design of a (so far presumably) safe Gaussian vault. First, the structural capacity considering the material properties shortly after the formwork is removed. At this point, the material strength has not had time to fully develop but the structure is exposed to the full load case. This should thus be used to determine appropriate funicular form between supports. The second condition to consider is capacity against non-uniform live load cases and the third is resistance against buckling.

Dead loads should be considered the dominant load case and thus used for design of the funicular thrust lines. This is appropriate because during most of the structural life cycle dead loads will be the only acting force and even including wind, dead loads are still dominant. Other live-load dominant load cases may be perceived such as snowfall or earthquake. Surely the vault could be designed for a uniform snow distribution but non-uniform snow distribution (and earthquake loads) are arguably too unpredictable to be used in design. Because of this Gaussian vault may not be an appropriate structure for areas with either heavy snowfall or earthquakes.

The material design properties for brickwork under hardening used by Dieste was an Elastic modulus of 7GPa and brick compressive strength of approximately 8MPa (Pedreschi and Theodossopoulos, 2007).

Once preliminary funicular thrust lines are determined for the uniform dominant load case, non-uniform load cases must be controlled. The structural capacity against non-uniform load cases is accounted for by a variation of Moseleys condition for arch stability (*“if a thrust line runs entirely inside the arch and the resultant at each joint lies within the friction cone, the arch is clearly stable”* (Moseley, 1843)). The variation of this condition posed by Allen and Zalewski (2010) argues that the vault is stable if a funicular per possible load cases may pass within the *middle one third of the vault undulation amplitude*. This condition will be analysed in the discussion.

Dieste produced design charts that may be used to determine the characteristic vault slenderness  $\chi$ , from which the characteristic buckling load may be determined by equation 2-5. To use the design charts one simply must determine the value  $\gamma$  as a function of the medium vault spring angle at supports and  $v$  the ration between moment of inertia at the crown and at supports.

$$(2) \quad \chi = \frac{ql^3}{EI}$$

$$(3) \quad \gamma = \frac{1}{\tan(\varphi_0)}$$

$$(4) \quad v = \frac{I_{crown}}{I_{support}}$$

$$(5) \quad I = \frac{l_s t h^2}{8} + \frac{b t^3}{12}$$

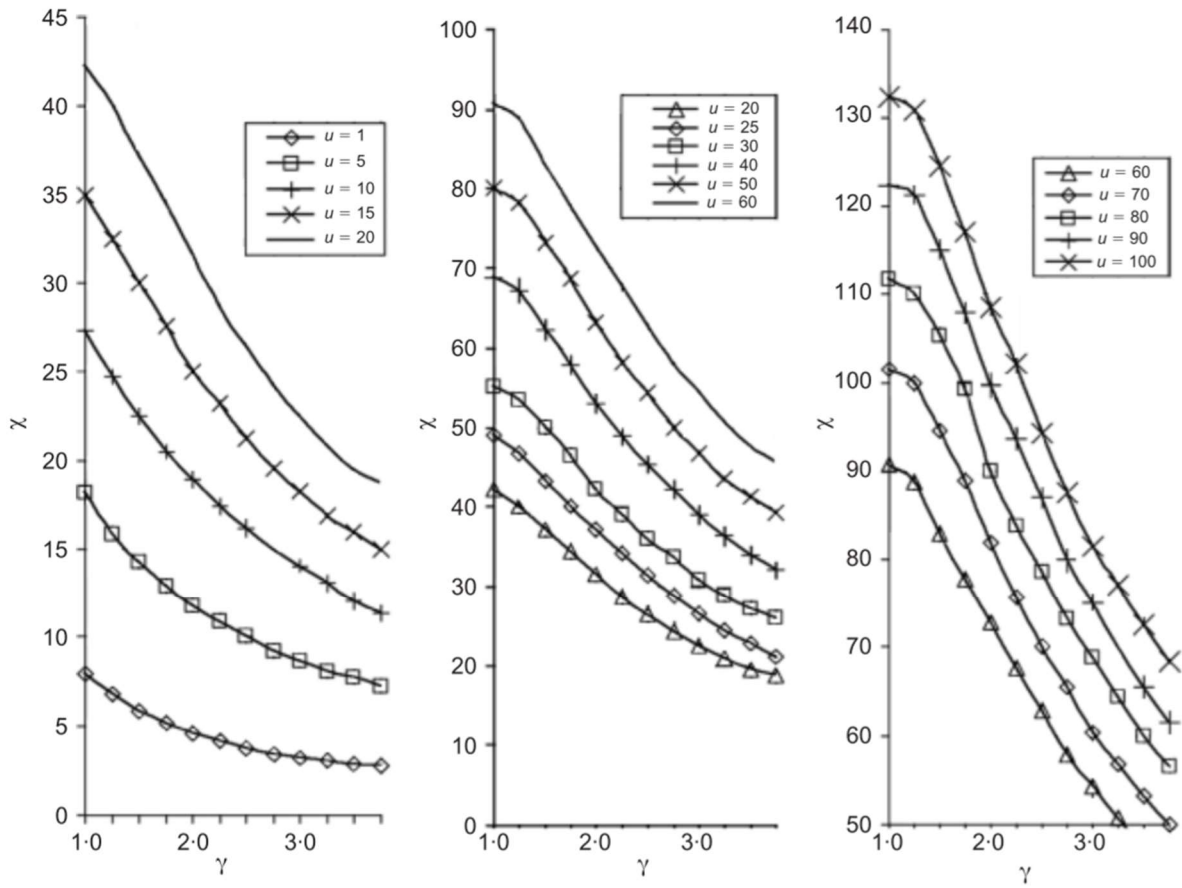


Figure 17. Design charts for buckling capacity of Gaussian vault.  
 (Source: Dieste, E. 1985. Ediciones de la banda oriental. Montevideo, Uruguay)

### 1.4.3 Case introduction

To illustrate the presented design procedure a Gaussian vault spanning 30 meter will be designed. Each vault will have an approximate width of 4m. The method could be used to explore architectural variation but this section will focus on one form like that of Diestes architecture. The structure is not site-specific but simply presumed to be exposed to design wind speed of 25 m/s. Snow and earthquake loads are not accounted for.

In Gaussian Vault design, it is perhaps more important to accurately determine the distribution of forces than it is to determine the precise magnitude of forces. In the graphic statics model the dead load force applied in each node should be

specific to each segment length. Due to the low vault rise, the non-uniform force distribution may be approximated to a uniform force distribution with only about 5% inaccuracy. Funiculars designed for true dead load distribution should have somewhat higher rise than produced with this model

A wide range of possible live-load distributions may be analysed for effect but it is here assumed that the worst case non-uniform load case is that when the wind hit with equal but opposite force perpendicular to leeward- and windward-side respectively, illustrated in figure 3.

Since wind is applied perpendicular to the surface, a surface needs to be assumed so that the wind may be applied perpendicular to it. Here, two different funiculars are assumed. One approximately representing the upper boundary of crown transverse undulation and the other representing the lower boundary.

The force magnitudes are estimated as a high boundary value. Pressure coefficients corresponding to an average roof angle of 15 degrees per Eurocode is  $C_{pe} +0,7$  windward side and  $-1,0$  leeward side worst case combination. This is a high bound estimate compared to proposed pressure coefficients proposed by Melbourne W. H, that is  $C_{pe} -0,5$  and  $+0,4$  (Melbourne, 1995).

As the wind pressure tends to quickly switch between pressure and suction it is appropriate to perform a detailed wind analysis before detailed design. Such an analysis should include the effects of vibrations.

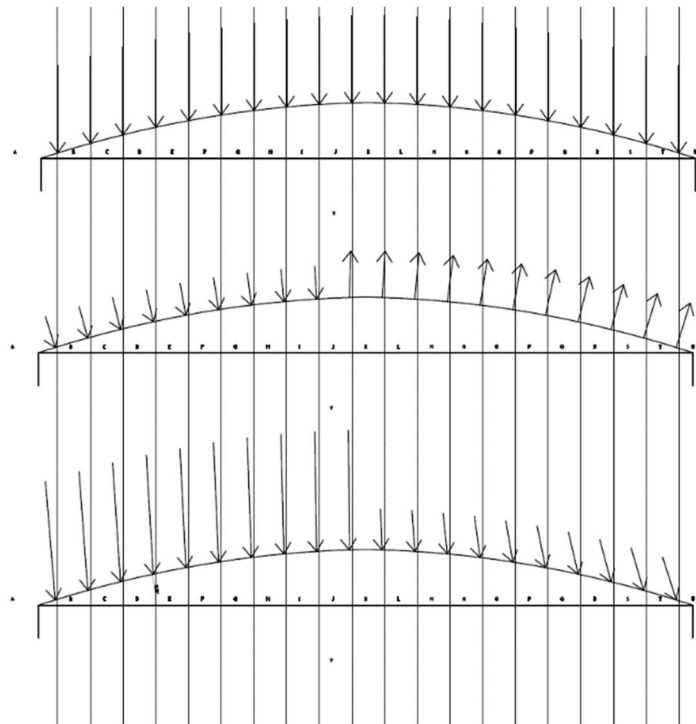


Figure 18, Force distribution. Dead load, wind load and resultant asymmetric combined load.

### 1.4.4 Design process

The vault is designed in iterations where the geometry is assumed, analysed and modified until satisfactory results are achieved. Initially, a transverse cross section somewhere along the length of the vault needs to be presumed. Using graphic statics, Wolfe’s method may be used to identify any number of funiculars intersecting both supports and the presumed cross section. From this simple geometric construct, all equation (2-5) variables may simply be measured. In this case, a crown transverse cross section is presumed.

The highest and the lowest rise funiculars are important variables to satisfy the middle 1/3 criteria for resistance capacity to asymmetric loads and the undulation should be designed accordingly. Here the lower boundary funicular is assumed with a span to rise ratio of 7:1 and upper boundary to 12:1. The assumptions are based on the most typical span to rise ratios of Diestes vaults; 7:1-10:1. The cross section presumed here is illustrated in figure 19.

All individual funiculars are despite varying rise presumed to be exposed to the same load distribution. This is a simplification and the preliminary funiculars should as such be recalculated with the appropriate loads before detailed design. However, for preliminary design it is a reasonable simplification.

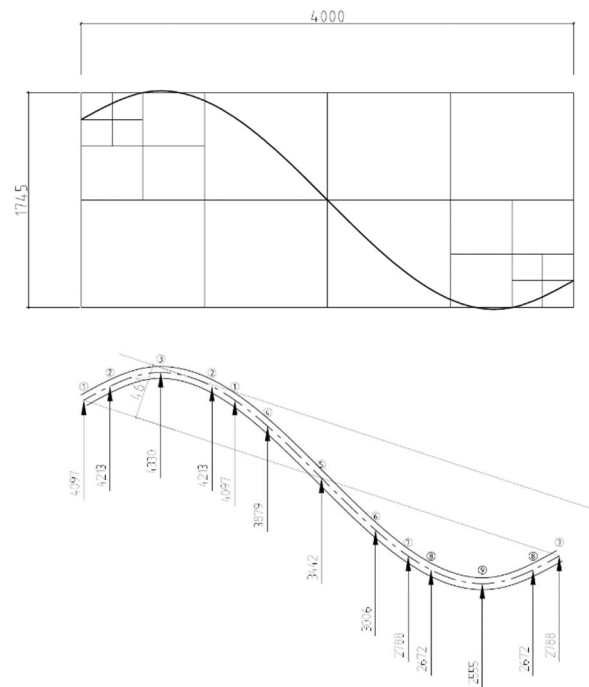


Figure 19. Presumed crown transverse undulation.

Funiculars are easily projected to 3D in a CAD environment, where the initial springing angle and section length at both support and crown may be measured. From the crown and support transverse sections, respective  $l_s$  and  $h$  is measured. For proposed design  $l_s$  measure 4,7m at the crown and 4,01m at supports with  $h$  measuring 0,46m at crown and -0m at supports. The spring angle  $\varphi_0$  is measured close to supports between funiculars and horizontal plane. Here angles vary between 18,8 to 30 degrees, with a weighted average of 24,5 degrees. The buckling capacity is calculated using the equations (2-5) and diagrams (figure 17) provided by Dieste.

Presuming a sufficiently large critical buckling load one may proceed and check the middle 1/3 criteria. It is an iterative process where an origo is assumed and tested for funicular compliance. The process may be solved as a constrained optimisation problem utilizing parametric design tools available in common CAD packages such as Autocad Architecture 2016 used here.

If Wolfe’s method is used to generate the funiculars, parametric constraints may be used to make the iterations quicker. ‘X’, ‘X’’, ‘Z’ and ‘Z’’ should be fixed positions. Lines ‘X-Y’ should intersect ‘Y-Z’ and ‘X’-Y’ should intersect ‘Y’-Z’’. ‘X-Y’ are constrained to be parallel with ‘X’-Y’ and ‘Y-Z’ constrained to be parallel with ‘Y’-Z’.

### 1.4.5 Results

Out of three conditions two are satisfied completely. Equilibrium under main determining load case is satisfied and so is resistance against buckling. The *middle 1/3* criteria for non-uniform load case equilibrium proved hard to satisfy.

Out of all the funicular thrust lines for the determining uniform load case, the stresses reach a maximum of 3.1 MPa (lower boundary thrust line at supports). That is a 2.5 factor of safety against material failure compared to a conservative brick compression failure design value of 8MPa.

Here the buckling load is calculated to 4kN/m as for a 1-meter wide strip. Compared to design uniform load of 3.5kN/m, that is a 1.14 factor of safety against buckling.

Fig 19 illustrates a *thrust zone* (hatched in figure) required to fit all non-uniform thrust lines with minimum variation in funicular rise over each transverse section. The thrust zone is the result of many iterations and a good approximation of best compliance with condition. Clearly only a small section of the thrust zone fit within the middle 1/3 of undulation and as such the condition is not satisfied. At the same time, the result illustrates that it is possible to fit even the worst-case non-uniform thrust lines within the boundary of the undulation.

The vault geometry is illustrated in fig 20 and case roof concept is presented in figure 22.

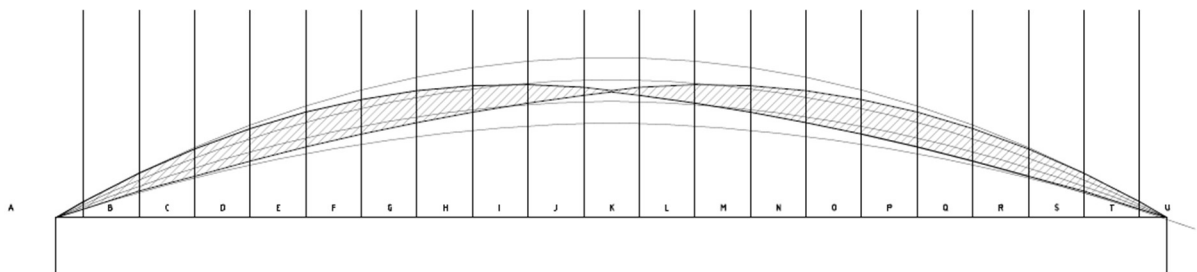


Figure 20. Minimum 'thrust zone'

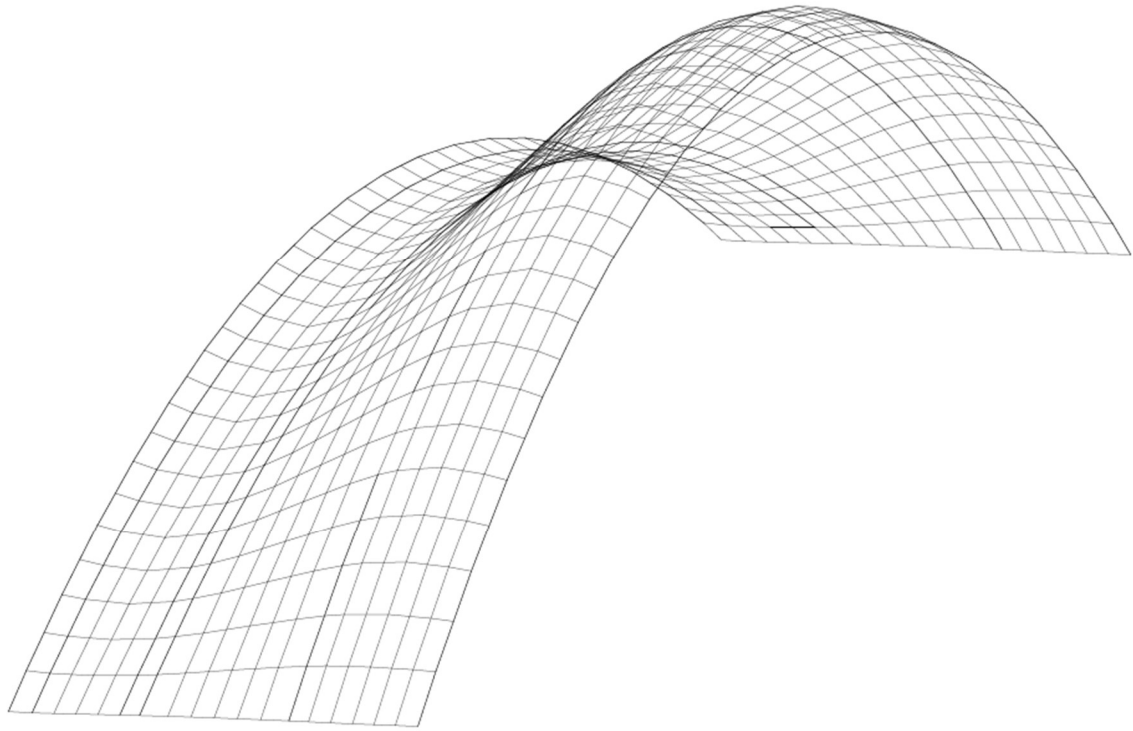


Figure 21. Gaussian vault geometry.

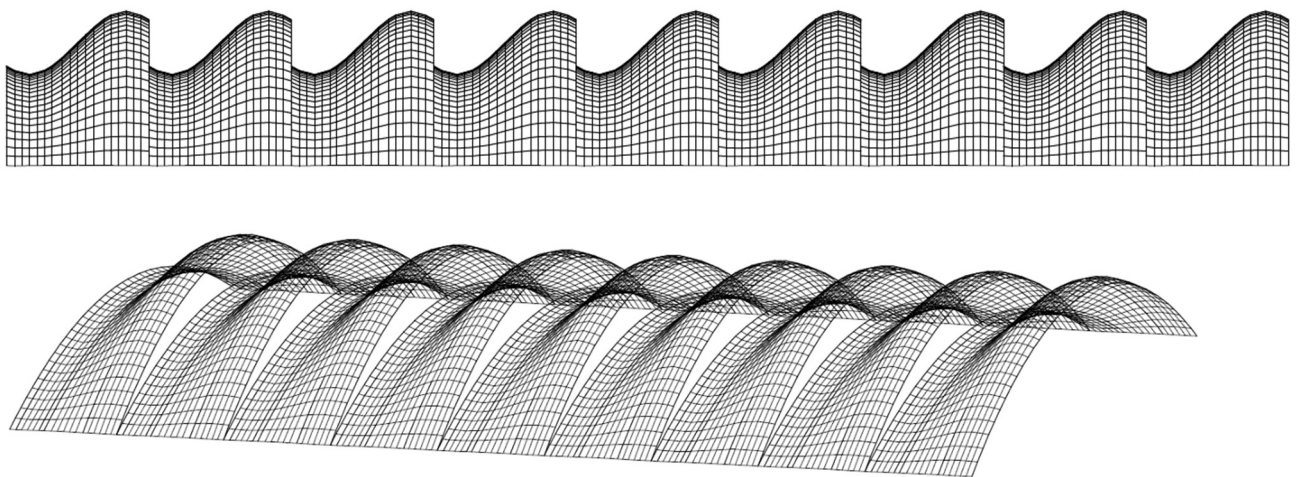


Figure 22. Perspectives on roof system

#### 1.4.6 Discussion of model

The purpose of this discussion is to bring to the attention the limitations of presented model. As any model, the presented one does not help predict reality but it is useful when designing a structure that will work. As George E.P Box famously stated, “All models are wrong, but some are useful”.

Gaussian vaults carry the loads that they are exposed to by funicular compressive thrust lines to the supports. Although compressive axial stresses are the primary type of stresses within the Gaussian structure, other types of stresses must occur to achieve equilibrium. To guarantee the structural safety it is necessary to include this aspect in analysis. Either explicitly by calculation or implicitly by proving the in-plane shear- and out of plane moment-forces can be neglected. In the presented method, these forces are implicitly assumed neglected on three occasions:

First, when constructing the Gaussian vault with the presented method it is assumed in the model that adjacent funiculars work in discrete independence of each other. Each longitudinal section is subject to, and determined by external loads alone. Yet, all theoretical funicular sections are part of a continuous material where no such discrete sectional boundaries exist. Any transverse section (other than an arbitrary horizontal line) is along its length subject to different levels of stress normal to its cross-section surface. Presented with varying normal stresses; shear forces should develop perpendicular to the transverse section surface.

The finite element analysis presented by (Pedreschi and Theodossopoulos, 2007) shows a significant difference in stress distribution compared to the stress distribution the studied structure was designed for. It is the interpretation of this thesis author that this stress distribution difference in part is due to FE-model allow stress redistribution by transverse and moment internal forces.

Second, when determining the moment of inertia for the crown and the support section it is assumed that all transverse sections work as a unit and stresses may be distributed within the section appropriately. Resistance against buckling is achieved by undulating the surface of the vault in the transverse direction and utilizing the cross-sectional moment of inertia. By Diestes equation, the moment of inertia is primarily determined by the thickness of the vault and the height of its undulation. Thus, it is assumed that the transverse cross section may be analysed as a unit. This assumption also relies on an assumed sufficient shear force capacity.

Last, it is assumed that if all the funicular thrust lines fit within the boundaries of the undulation, the structure will be in equilibrium. This assumption is in conflict the principle of thrust lines. The uniform thrust lines, on which the geometry is based, are symmetrical. The non-uniform load cases, such as those including wind, are asymmetric. To simply fit an asymmetric thrust line ‘within the undulation of the structure’ is not an easy task. Either the asymmetric thrust line may be found on a diagonal within the structure or other modes of action than thrust lines are relied upon to achieve equilibrium for the non-uniform load case.

The capacity for in-plane shear and out of plane moment for masonry structures are well documented and proved significant (In plane shear and out of plane bending capacity interaction in brick masonry walls). It is beyond the scope of this thesis to apply these related studies to presented model.

### 1.4.7 Discussion of results

Satisfying the requirement posed by Zalewski and Allen (2010) proves close to impossible due to the simultaneous practical restriction on feasible vault rise. The two restrictions are not easily consolidated and thus the presented method is severely limited if both these rules are to be followed completely. It may be the case that both rules do not need to be abided precisely but that they may be taken as guiding principles and supplemented by case by case conclusions.

In this case, it is the opinion of this thesis author that the middle one third rule may be considered a flexible recommendation. The rule and the reasoning behind this opinion should however be properly analysed before forming conclusions. The reasoning is presented in purpose to inspire constructive criticism of presented method and also to inspire future development.

To illustrate a flexible interpretation of the rule three transverse sections are considered. One on windward side, one at the crown and one on the leeward side. On the windward side, it is appropriate that the non-uniform thrust line tangent the upper boundary as the wind hits the upper boundary the hardest. A transverse section at the crown of the vault is also appropriately passed mid height of the undulation at an intersection with the structure. On the leeward side, the non-symmetry funicular passes through the lower part of the transverse section, close to the lower boundary undulation. Thus, non-uniform thrust lines may be able to form on a diagonal across the vault.

Irrespective of if the rule should be considered as strict or a flexible recommendation, the conflict does illustrate an important point where the model does not accurately predict the structural behaviour. It may still accurately predict structural safety.

The true structural behaviour is very likely to include stresses other than compressive in the longitudinal direction. To resist non-uniform loads, the vault must distribute the stresses to the stiffest path between supports. This distribution requires in-plane shear and out of plane moments. This complexity effectively must be comprised within the predictions of simplistic the middle one third rule.

If in-plane shear and out of plane moments may be recruited to achieve equilibrium under non-uniform load cases, then the presented non-uniform thrust zone may be argued to predict a safe structural behaviour. Although argument should be proved.

The designed vault has a larger rise and deeper undulation than Diestes as presented in (Pedreschi, and Theodossopoulos, 2007). This would explain the, in comparison, large buckling load – since undulation is the main variable for buckling resistance. This difference should be properly examined so that the increased transverse angles does not inexplicitly violate any preconditions for calculations.



# PART II

## FUTURE GRAPHIC STATICS



## 2.1 Introduction

The following section will introduce two pioneering examples of modern structural exploration research utilizing Graphic statics.

As head engineer of leading design firm *Skidmore, Owings & Merrill*, William F. Baker is responsible for some of the world's most extreme structures such as the Burj Khalifa. Constantly searching for ways to push the limits of high-performance structures, the need for structural exploration and performance optimisation naturally arises. In *Structural exploration using graphic statics* (Beghini, 2013), the authors (including Baker) present an optimisation method intended to solve otherwise complex optimisation problems and to expand the possible design space. The presented tool utilizes the graphic statics reciprocal relationship between form and force, to optimise using force domain variables.

*Digital structures* group led by Caitlin Mueller at MIT are pioneering algorithms that apply computational genetic evolution to design of structures. Evolutionary algorithms are a general computational strategy mimicking the biological evolutionary selection process for optimisation and computer learning. The intention of the presented tool is to integrate preliminary analysis and design and inspire alternative forms. The tool allows structures to be generated and evaluated on a complex set of criteria combining architectural and engineering priorities.

## 2.2 Structural optimization using graphic statics

According to Baker, a structure may be defined on three system levels of detail (Baker, 2015). In the most detailed level; the *size* of structural members is considered and designed. This is the lowest level of influence on the performance of the structure because of its marginal effect on the distribution of forces within the structure. On the holistic level; the *topology* of a structure is considered and designed. The topology describes for example the boundaries, number of nodes and connectivity in a frame, or the number of supports and extension of a plate. This is the highest level of influence on the performance. In the intermediate level is the *shape* of a structure. Using the same examples, the shape would describe the position of the nodes in a frame or the position of supports under a plate.

Baker's theoretical studies and practical work both show the importance of engineering the topology and shape of a structure. In *Connecting architecture and engineering through structural topology optimisation* (Beghini, 2014) the authors discuss the importance of close discipline cooperation where engineers join the exploration of structural form. It is the perspective of Beghini et.al. that cross-discipline projects may either result in a project where neither is satisfied with the result or one where synergy is achieved and the result is better than what either discipline may have managed on its own. It is his view that synergistic results are achieved in close discipline collaboration where structure is explored together and respective perspective and ideas inform and enforce the each other's work (Beghini, 2014).

Topology optimisation tools are effective as means of enhancing the *interactive rational process* where architects and engineers may more effectively incorporate each other's ideas where they have the best effect. Thus, achieving synergistic results (Beghini, 2014)

In *Structural optimisation using graphic statics* (Beghini, 2013) the authors present a topology optimisation strategy utilizing the Graphic statics model. Building the optimisation algorithm on the Graphic statics model has several interesting advantages compared to algorithms building on a Finite elements model (as is common).

Where most optimisation methods use form domain variables, it is possible with Graphic statics model to use force domain variables. Partly the benefit of force domain optimisation relates to decreased processing time. Force domain optimisation tend to require less variables than form domain (Beghini, 2013). It is therefore possible to use the saved processing time to explore more structure alternatives or larger structures. As the processing time usually increase exponentially with the number of variables, this is a significant benefit.

Perhaps the primary benefit of force domain optimisation using graphic statics relates to maintaining equilibrium during exploration. Subject to the constraints of reciprocity, a structure will always be in equilibrium while all force graph polygons are closed. Optimising with force graph nodes as variables, resulting structure will always satisfy equilibrium (if initial structure satisfies equilibrium).

The principles relating form and forces in a Finite element model are by comparison much more complex and linear from form to force. By optimising the form of a FE model, it is possible that resulting forces are not in equilibrium.

Readers are referred to “*Connecting architecture and engineering through structural topology optimisation*” and “*Structural optimisation using Graphic statics*” for introduction to common topology optimisation tools and methods and full comparison.

Many optimal design problems concern primarily axial member structures (Beghini, 2013). Such structures may not necessarily be fully triangulated as the flexural stiffness provide sufficient stiffness to the structure, making it stable. Yet it is necessary to triangulate the geometry in the model or the model structure may become numerically “unstable”. Numerically unstable structures often result

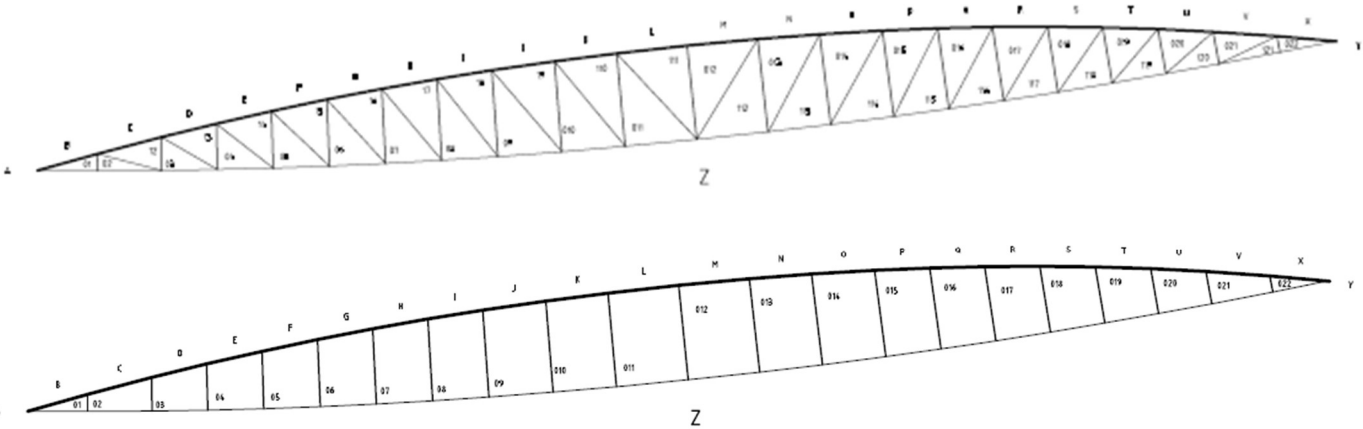


Figure 23. Triangulated lenticular truss (top). “Unstable” lenticular truss (bottom)

in a singular finite element stiffness matrix, and as such the equilibrium equations may be unsolvable.

The paradox of stable yet ‘unstable’ structures may be illustrated by studying the force graph belonging to the lenticular truss in figure 23 (top). The truss is subject to a uniform load applied to the top chord.

The force graph reveals that the triangulating web members are not subjected to any force. Individual force polygons are read by following a clockwise orientation around the studied node. K connects to L, that connects to 111 but no edge connecting to 011 is visible. This is because the length of diagonal member 111-011 is zero in the force graph.

The lenticular truss could as such be reduced as illustrated in figure 23 (bottom). In theory, this truss is optimal and stable for exact load case but unstable for any other load case. Modelling a stable yet ‘unstable’ structure might seem unpractical but as it serves a purpose in preliminary design.

When generating and optimising in preliminary design it is beneficial to design per a single dominant load case. This may result in a structure that is unstable for any other load case. Which is why in detailed design it is essential to consider all relevant load cases and reinforce structure where needed. In detailed design, it may be necessary to consider torsional capacity or even add additional members. Non-the less, structures optimised for dominant load case alone tend to be very efficient (Beghini, 2013).

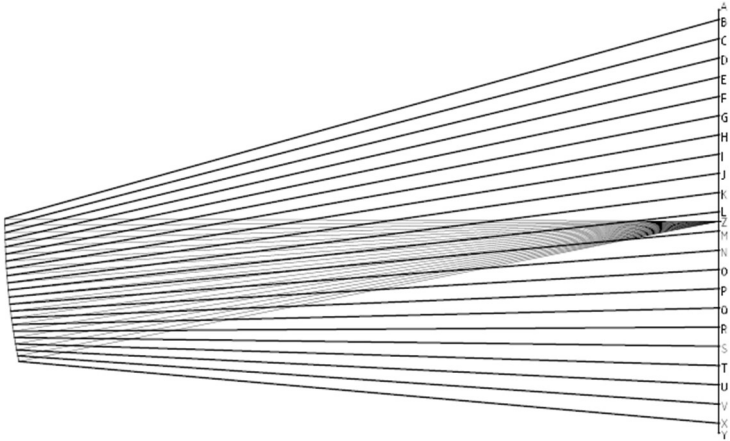


Figure 24. Force graph of triangulated lenticular truss.

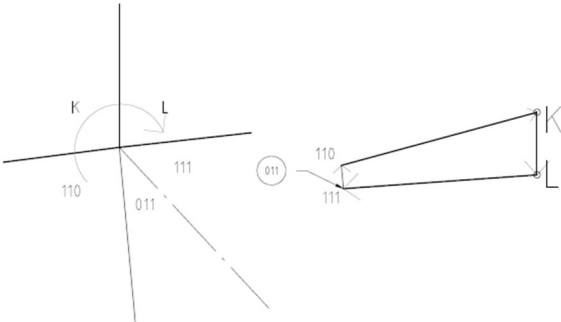


Figure 25. Individual node and reciprocal force polygon.

In *Structural optimisation using Graphic statics*, authors present a simple six step process for structural optimisation utilizing the graphic statics force domain, as follows:

1. Given a specified general geometry and connectivity of a structure (form diagram), draw the corresponding reciprocal force diagram. Determine which node degrees of freedom in force diagram are restrained.
2. Assign design variables to each node degree of freedom in force diagram that is not restrained by reciprocal relationships.
3. Compute the sensitivities of the design variables (if necessary) and update the design variables using suitable optimisation algorithm.
4. Update the reciprocal force diagram, and use this to construct new form graph.
5. Calculate the length of the lines in both diagrams.
6. Calculate the objective function based on the line lengths and repeat until convergence is achieved.

A project utilizing the force domain structural optimisation is illustrated in *Structural optimisation using Graphic statics*. The example applies the optimisation process to a large span truss. The example truss is part of a series of trusses intended to carry the load of a large convention centre roof as expressive parts of the architecture. Each truss span a total of 162m resting on two supports. Main span is 90m and two cantilevers on each side reach 45m and 27m respectively. Dominant load case is assumed uniform.

Several alternative truss topologies were considered in a preliminary study. It was concluded that a 9-meter-deep truss with X-bracing web members (figure 26a) was approximately optimal for the problem and applicable as initial layout for optimisation.

The pursued optimum is minimum of total steel volume. Assuming constant stress the objective function is formulated with equation 6, where  $L$  and  $L^*$  are form and force edge lengths

$$(6) \quad \min_x V = \min_x V \frac{1}{\sigma} \sum L_i L_i^*$$

To account for buckling, the allowable compressive stress was calculated each iteration considering the slenderness of each member. Total steel volume could thus be calculated each iteration as the sum of individual member internal force divided by allowable stress.

The form graph constraints allow the user to experiment with different shapes. Only the bottom chord of the truss was initially constrained. This resulted in a baseline optimum truss with only 55% of the steel volume compared to original X-braced truss.

Optimum structures often correspond to irrational structures that neither satisfy architectural or constructability criteria. Unconstrained base-line truss is very efficient but entirely unpractical. It is possible to explore efficient alternatives experimenting with constraints that may also satisfy architectural and constructability criteria. Some alternative constraint set ups and resulting structural volume explored by Baker and team are illustrated in figure 26 b-e. Alternative 'e' is selected as proposed preliminary design.

The proposed design will require further analysis in detailed design. As described the process only considers a single assumed dominant load case, it is critical that the proposed design is analysed for possible asymmetric load cases. The detailed analysis will likely require some members to be upsized and possibly even adding some member for increased redundancy. However, it is the experience of Baker and fellow authors that these additions are marginal on total structural volume. It is as such concluded that optimising the preliminary structure for a dominant load case does result in very efficient and rigid structures.

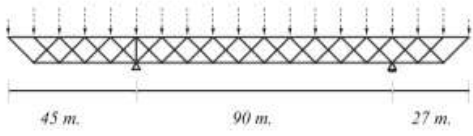
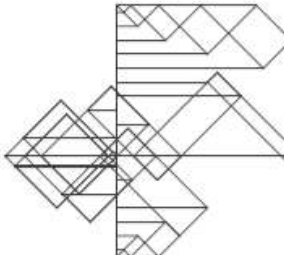
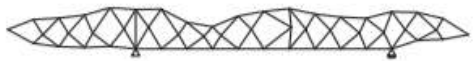
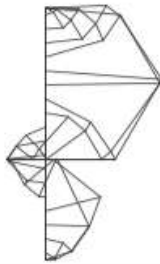
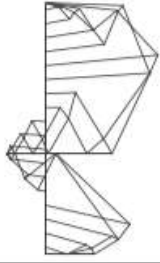
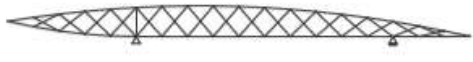
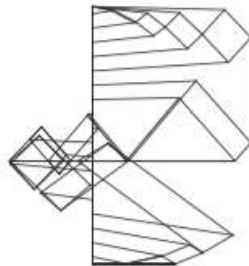
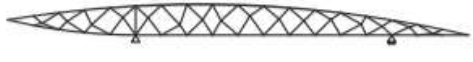
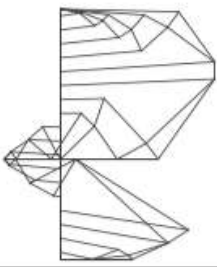
Description	Form Diagram	Force Diagram	Normalized Volume
(a) Initial truss connectivity			1.000
(b) Benchmark truss; top chord, cantilevers and web members unconstrained			0.552
(c) Chord profiles constrained for architectural and functional reasons			0.629
(d) Depth constrained, straight web members (X-diagonals)			0.852
(e) Depth constrained			0.669

Figure 26. Design alternatives developed for a long span-truss. (Source: Beghini, 2013)

## 2.3 Evolutionary design space exploration

As Mueller and Ochsendorf explain in *Combining structural performance and designer preferences in evolutionary design space exploration* (2015), designers must consider a wide range of goals for their intended design. They define some criteria as ‘quantifiable’. Such as amount of material, costs etc. Quantifiable criteria are relatively easy to implement in a computer optimization algorithm. Some criteria are not quantifiable but rather ‘qualitative’. They define qualitative criteria to include such criteria as aesthetics, constructability and contextual appropriateness. These criteria are hard to encode in algorithms and would usually require human evaluation. Their evolutionary algorithms are part hard coded optimisation on quantifiable criteria and part user driven selection process on qualitative criteria.

It is also the view of Mueller and Ochsendorf that an important aspect of the design process is how the process itself influences the direction of development. One may set out with an initial design idea but during the process of exploring that idea may very well give birth to alternative related ideas worth exploring. A truly empowering design tool should as such encourage the pursuit of alternative related design ideas.

The team has developed a tool called *StructureFIT* that combines the optimisation and exploration aspect of the design process. Integrating evolutionary algorithms *StructureFIT* encourages the designer to explore a wide range of alternative structures and to find to ones best suited for intended use.

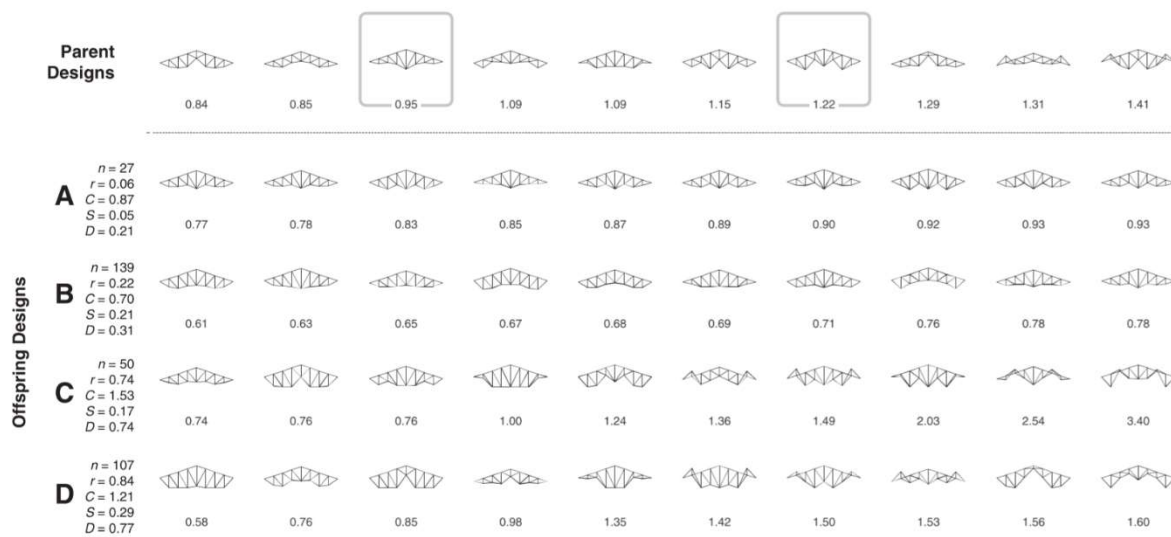


Figure 27. Screen capture from *StructureFIT* illustrating design generations and selection. (Source: Mueller and Ochsendorf, 2015)

In analogy with how the random genetic mutation of DNA sometimes produces successful new properties in organisms, the structural geometries may be mutated at random to explore possible alternatives. As with genetic evolution, digital genetic evolution will usually produce unsuccessful mutations but every so often something brilliant evolves.

The strategy used by Mueller and Ochsendorf implements five steps in repeat to mimic the evolutionary mutation process. First, a generation of design alternatives are produced from seed designs. Second, the generation is analysed for the quantifiable criteria. In a lucky evolution, the user may at this stage be satisfied with the alternatives provided and would thus be allowed to end the selection process. If not satisfied, the user will select favourite alternatives (on qualitative criteria) which will become the parent generation of next iteration. Continuous mutation and selection will over several generations evolve the structures towards a more desirable optimal design.

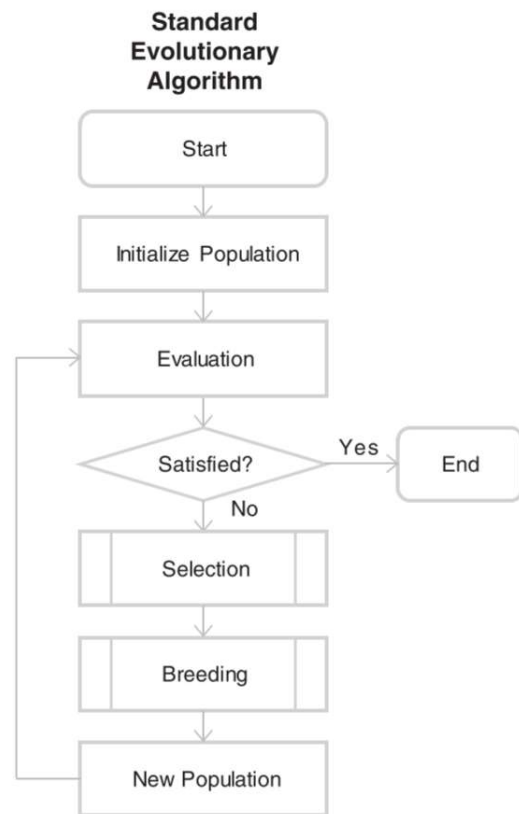


Figure 28. Proposed standard evolutionary algorithm. (Source: Mueller and Ochsendorf, 2015)

In the selection phase of their digital evolution strategy, the user is allowed to actively modify the generated structures as desired before progressing with the evolution. The breeding phase also includes features to modify the breeding stage by manipulating the generation size and mutation frequency.

Their case studies show that low mutation rate combined with large generation sizes set up the evolution for generating high performing designs close in appearance to the initial design. This set up is ideal when optimising on hard factors such as cost or performance. Their case studies also show that smaller generation sizes combined with high mutation rate set up the evolution for generating imaginative designs with similar or slightly better structural performance compared to initial design.

To illustrate the potential of each approach, design variations of a frame (figure 30) are produced each using either a performance optimisation approach, a hybrid approach or a free form exploration.

It is their conclusion that in practice, a hybrid design approach combining medium mutation rates and large generation sizes are likely the most useful approach. In the selection phase the user selects variations on both structural performance and qualitative aspects. This is likely to produce design offspring that resemble the initial design but perform significantly better. Thus, providing

structures in line with the architect's intentions but that require significantly less materials or cost less.

Illustrated in figure 31 are the design generations of the hybrid approach and the selected alternatives for each generation. From a population of 90 alternatives, the top then performing alternatives are pictured. Note that the alternatives featuring the top performance are not immediately selected as seeds for next generation. Rather the alternatives judged as acceptable performance and featuring desirable qualities are selected as seeds for next generation.

By the first few generations the mutation rate is relatively high to produce variation. From the generated variations, desirable design directions are selected as seeds. When approximate desirable forms designs have been achieved, the mutation rate is decreased for a few generations while alternatives are selected for performance.

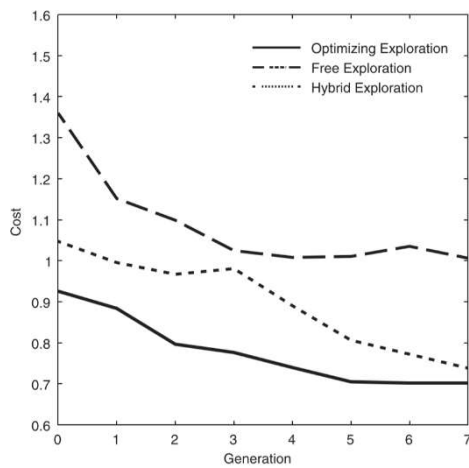


Figure 29. Comparison of structural efficiency over evolution. (Source: Mueller and Ochsendorf, 2015)

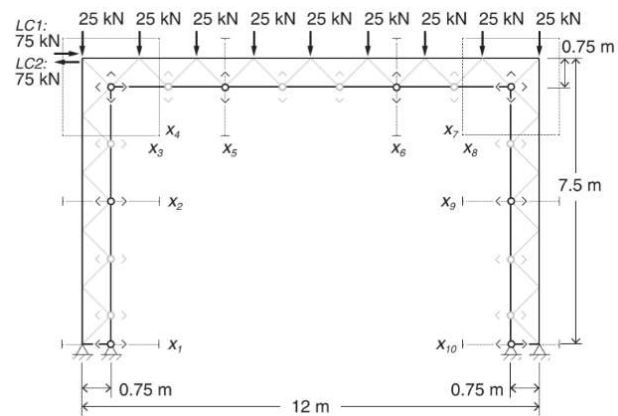


Figure 30. (Source: Mueller and Ochsendorf, 2015)

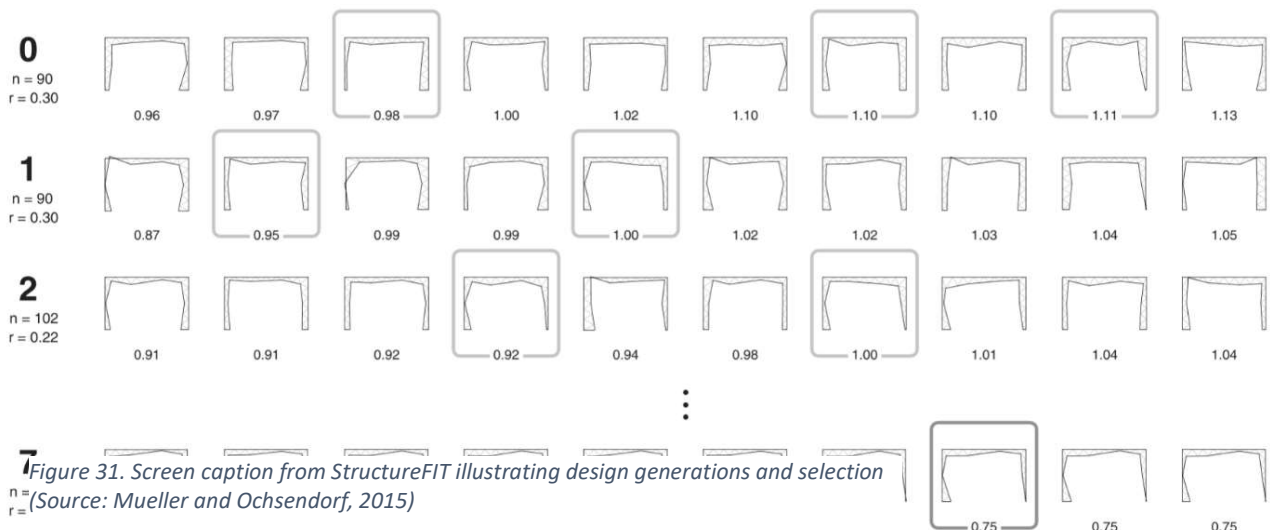


Figure 31. Screen caption from StructureFIT illustrating design generations and selection (Source: Mueller and Ochsendorf, 2015)

## 2.4 Discussion

It is concluded by Mueller and Ochsendorf that the future work to develop the method further should focus on including more quantitative goals in the optimisation process. They suggest further focus on energy, daylight performance, constructability and embodied energy.

An interesting aspect of the constructability goal is the translation from conceptual structural model to detailed structural design model. Obviously, a frame model is ideal for frames such as the one presented in the hybrid example. The preliminary model is directly applicable in detailed design analysis. Yet the illustrated structures resulting from the hybrid design exploration (figure 32) are reinforced concrete frames. The detailed analysis model is not in perfect analogy with the frame model. Aligning the preliminary design model with the detailed design model is a key factor of the constructability goal.

As model complexity is prone to produce design errors and significant project costs, complexity is usually avoided in practice in favour of simplistic upper boundary models. As the full complexity of the intended design is reduced to practical upper boundary models it is often desired to change the intended design to fit the desired model. Thus, expressive structures risk degradation if not designed in alignment with the requirements of analysis model and constructability principles.

Important questions to consider for constructability evaluation strategy are; how would one automatically evaluate the complexity of a detailed analysis based on the conceptual model?

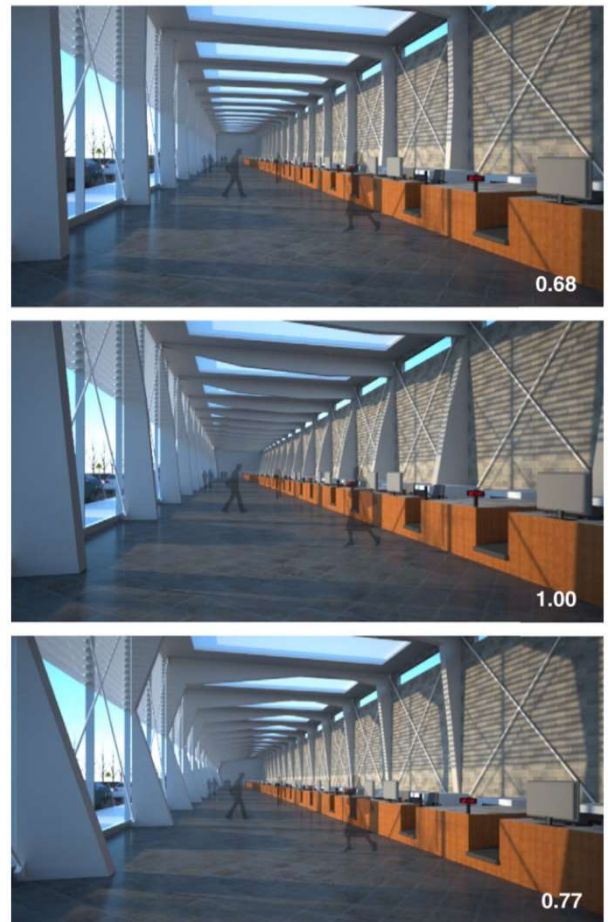


Figure 32. Result of hybrid design exploration.  
(Source: Mueller and Ochsendorf, 2015)



**PART III**  
COMPUTATIONAL GRAPHIC STATICS



### 3.1 Introduction

As illustrated by the examples in first and second part of this thesis, graphic statics is useful in both the original form and as a computerised model. By computer implementation it is possible to enhance and extend the capabilities of graphic statics by integration with other software based methods. As illustrated in second part of this thesis, one such synergy is found by extending graphic statics form finding capabilities with optimisation algorithms.

The computer implementation of the graphic statics requires a reinterpretation of graphic geometry to a format that may be processed by algorithms. Different implementation strategies are possible. Currently two approaches are competing for popularity.

*A fully geometric approach to interactive constraint based structural equilibrium design* (Fivet and Zastavni, 2014) present one approach. This approach has topology represented by five types of geometric data sets; points, constraints, Boolean constraints, forces and rods. From this data construction, it is possible to interactively create form and force graphs from either domain.

The algebraic approach is examined in this thesis. The algebraic approach has topology represented by matrices and reciprocity constraints solved by algebraic equations. This approach allows form to force interactive manipulation without breaking the reciprocal relationship. This approach is presented by Tom Van Mele and Philippe Block in *Algebraic Graphic statics* (2014). It is their specific strategy and algorithm that is examined in following section

The algebraic approach is in the following section presented as applied to the suspension bridge previously studied in first part of this thesis. Topological representation and reciprocity calculations using algebra should be presented. A strategy for user interface integration is proposed by this author and explored as a proof of concept.

### 3.2 Definitions

The *dual* of a graph is a graph that has a node for every surface of the original. The *dual* nodes are connected by an edge whenever corresponding surfaces in the original share a separating edge.

Form and force graph are referred to as  $G$  and  $G^*$  respectively.

Graph *connectivity* refers to how edges are connected between graph nodes. Matrix  $C$  represents the directed connectivity of form graph.  $C^*$  represent the directed connectivity of force graph.

### 3.3 Algebraic graph representation

The first stage of the setup is the construction of connectivity matrices. The second is that vectors containing node coordinates should be constructed.

Initially, nodes, edges and surfaces need to be indexed. Each type is indexed by its own system. No particular indexation order is necessary but a systemised approach is strongly recommended. In addition to surface index a positive cycle direction should be defined. Here clockwise is used.

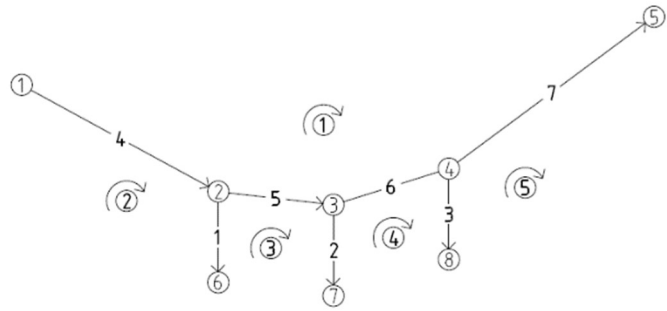


Figure 33. Bow's notation applied to form graph.

From edge and node index, edge direction may be defined. In theory, the direction may be defined arbitrarily but for clarity Block proposes a direction convention. Proposed direction convention has low index node as edge tail and high index node as edge head. This is used in following example.

Due to their defined dual relationship, both  $\mathbf{C}$  and  $\mathbf{C}^*$  may be constructed from an indexed form graph. In addition to encoding the connectivity of form and force graphs, the matrices also encode the edge direction following the definitions (6) and (7) respectively. Traversed refer to the reading the enclosing edges around a surface. Edges are read in turn of the defined cycle direction.

$$(6) \quad C_{ij} = \begin{cases} +1 & \text{if vertex is head of edge } j \\ -1 & \text{if vertex is tail of edge } j \\ 0 & \text{otherwise} \end{cases}$$

$$(7) \quad C_{ij}^* = \begin{cases} +1 & \text{if edge } j \text{ is traversed in the same direction as its orientation} \\ -1 & \text{if edge } j \text{ is traversed in opposite direction as its orientation} \\ 0 & \text{otherwise} \end{cases}$$

The resulting matrix structures are of size  $[v \times e]$  and  $[v^* \times e]$  where  $v^*$  is the number of form graph surfaces as well as the number of force graph nodes. A third connectivity matrix is constructed to represent the connectivity of only the internal nodes in force graph. This is simply constructed by extracting rows corresponding to internal edges from  $\mathbf{C}$ . Correct set up of example case will produce matrices as presented below.

$$\begin{array}{l}
\mathbf{C} \\
[\mathbf{v} \ \mathbf{x} \ \mathbf{e}]
\end{array}
\begin{array}{cccccc}
0 & 0 & 0 & -1 & 0 & 0 & 0 \\
-1 & 0 & 0 & 1 & -1 & 0 & 0 \\
0 & -1 & 0 & 0 & 1 & -1 & 0 \\
0 & 0 & -1 & 0 & 0 & 1 & -1 \\
0 & 0 & 0 & 0 & 0 & 0 & 1 \\
1 & 0 & 0 & 0 & 0 & 0 & 0 \\
0 & 1 & 0 & 0 & 0 & 0 & 0 \\
0 & 0 & 1 & 0 & 0 & 0 & 0
\end{array}$$

$$\begin{array}{l}
\mathbf{C}^* \\
[\mathbf{v}^* \ \mathbf{x} \ \mathbf{e}]
\end{array}
\begin{array}{cccccc}
0 & 0 & 0 & -1 & -1 & -1 & -1 \\
1 & 0 & 0 & 1 & 0 & 0 & 0 \\
-1 & 1 & 0 & 0 & 1 & 0 & 0 \\
0 & -1 & 1 & 0 & 0 & 1 & 0 \\
0 & 0 & -1 & 0 & 0 & 0 & 1
\end{array}$$

$$\begin{array}{l}
\mathbf{C}_i \\
[\mathbf{v}_i \ \mathbf{x} \ \mathbf{e}]
\end{array}
\begin{array}{cccccc}
-1 & 0 & 0 & 1 & -1 & 0 & 0 \\
0 & -1 & 0 & 0 & 1 & -1 & 0 \\
0 & 0 & -1 & 0 & 0 & 1 & -1
\end{array}$$

Node coordinate vectors  $\mathbf{x}$  and  $\mathbf{y}$  represent defined form graph node positions. Coordinates may be defined as absolute position or normalised position, as only relative position is of interest. From node coordinates it is important to note drawing scale as this is essential to determine force magnitude later.

### 3.4 Reciprocity and equilibrium conditions

Two conditions should be encoded in the algebraic transformation calculation. The first condition requires the dual force graph polygon to be closed if corresponding form graph node is in equilibrium. This is algebraically encoded such as the vector sum of each force graph polygon to equal zero. Second, corresponding edges should be parallel between form and force graph. As graphs are dual by set up definition, second conditions effectively graph reciprocity if satisfied.

Vector sum of each respective force polygon may be calculated as  $\mathbf{C}_i \mathbf{u}^*$  for x-axis and  $\mathbf{C}_i \mathbf{v}^*$  for y-axis. The vectors  $\mathbf{u}^*$  and  $\mathbf{v}^*$  as well as  $\mathbf{u}$  and  $\mathbf{v}$  are referred to as *coordinate difference vectors*. System equilibrium (and first condition) is satisfied if equation 8 is satisfied.

$$(8) \quad \begin{cases} \mathbf{C}_i \mathbf{u}^* = 0 \\ \mathbf{C}_i \mathbf{v}^* = 0 \end{cases}$$

The parallel edge constraint may be algebraically represented as equation 9, where  $\mathbf{Q}$  is a diagonal matrix encoding the *edge length differences*. Edge length difference may also be referred to as *force density*.

$$(9) \quad \begin{cases} \mathbf{u}^* = \mathbf{Q} \mathbf{u} \\ \mathbf{v}^* = \mathbf{Q} \mathbf{v} \end{cases}$$

$\mathbf{u}^*$  and  $\mathbf{v}^*$  are initially unknown and in fact the solution objective. When these are identified, the force graph node coordinates may simply be calculated by solving equation 11 and 12 for  $\mathbf{x}^*$  and  $\mathbf{y}^*$  respectively.

$$(10) \quad \mathbf{u}^* = \mathbf{C}^{*t} \mathbf{x}^*$$

$$(11) \quad \mathbf{v}^* = \mathbf{C}^{*t} \mathbf{y}^*$$

To identify  $\mathbf{u}^*$  and  $\mathbf{v}^*$  an *equilibrium equation* is formulated and solved. Combining both reciprocal condition equations 8 and 9. Using  $\mathbf{Q}\mathbf{u} = \mathbf{U}\mathbf{q}$  and  $\mathbf{Q}\mathbf{v} = \mathbf{V}\mathbf{q}$ , where  $\mathbf{U}$  and  $\mathbf{V}$  are the diagonal matrices of  $\mathbf{u}$  and  $\mathbf{v}$  equilibrium equation 13 may be formulated.

$$(12) \quad \begin{cases} \mathbf{C}_i \mathbf{U} \mathbf{q} = \mathbf{0} \\ \mathbf{C}_i \mathbf{V} \mathbf{q} = \mathbf{0} \end{cases}$$

Or,

$$(13) \quad \mathbf{A} \mathbf{q} = \mathbf{0} \quad \text{where} \quad \mathbf{A} = \begin{bmatrix} \mathbf{C}_i \mathbf{U} \\ \mathbf{C}_i \mathbf{V} \end{bmatrix}$$

$\mathbf{A}$  is referred to as the *equilibrium matrix* and  $\mathbf{q}$  referred to as the *force density vector* (or edge length difference vector).  $\mathbf{U}$  and  $\mathbf{V}$  are constructed as the diagonal matrices of  $\mathbf{u}$  and  $\mathbf{v}$ . This is found by equations 14 and 15. With  $\mathbf{C}_i$ ,  $\mathbf{U}$  and  $\mathbf{V}$  known;  $\mathbf{A}$  may be constructed.

$$(14) \quad \mathbf{u} = \mathbf{C}^t \mathbf{x}$$

$$(15) \quad \mathbf{v} = \mathbf{C}^t \mathbf{y}$$

$\mathbf{u}$	0	$\mathbf{v}$	-2954	$\mathbf{x}$	0	$\mathbf{y}$	13748
$[\mathbf{e} \times 1]$	0	$[\mathbf{e} \times 1]$	-2954	$[\mathbf{v} \times 1]$	6379	$[\mathbf{v} \times 1]$	10285
	0		-2954		10129		9856
	6379		-3463		13879		11028
	3750		-429		20541		15954
	3750		1172		6379		7331
	6662		4926		10129		6902
					13879		8074

$$\mathbf{A} \quad [2v_i * e]$$

0	0	0	6379	-3750	0	0
0	0	0	0	3750	-3750	0
0	0	0	0	0	3750	-6662
2954	0	0	-3463	429	0	0
0	2954	0	0	-429	-1172	0
0	0	2954	0	0	1172	-4926

Solving the equilibrium equation  $\mathbf{A}\mathbf{q} = \mathbf{0}$  requires different methodology depending on the shape of the system. Solution methodology is discussed in detail by authors in *Algebraic graphic statics* (2014).

With connectivity matrices, form coordinates and force density vector defined and identified,  $\mathbf{G}^*$  node coordinates may be identified by solving equations 10 and 11 for  $\mathbf{x}^*$  and  $\mathbf{y}^*$ . Due to algebraic complexities, the equation may not be solved directly but are first transformed to equation 16 and 17 where  $\mathbf{L}^* = \mathbf{C}^* \mathbf{C}^{*t}$ .

$$(16) \quad L^* x^* = Qu$$

$$(17) \quad L^* y^* = Qv$$

$$L \quad \begin{matrix} 4 & -1 & -1 & -1 & -1 \\ [v \ x \ v] & -1 & 2 & -1 & 0 & 0 \\ & -1 & -1 & 3 & -1 & 0 \\ & -1 & 0 & -1 & 3 & -1 \\ & -1 & 0 & 0 & -1 & 2 \end{matrix}$$

### 3.5 System self-stress and independent edges

An important aspect of the equilibrium equation is that it does not differentiate between internal edges and external forces. Both are simply treated equally as edges. As such the equilibrium matrix encodes both structure and external forces equally as ‘structure’.

Forces are introduced into the system through so called *system self-stress*. System self-stress may be understood in analogy with a steel truss where specific members are heated so that they expand. The expansion causes connecting joints to adapt a new state of equilibrium where force exerted by expanding member cause resultant forces in adjacent members. Because of the expansion, the system is in an induced state of self-stress. Analogous to heating a structural member, system self-stress can be induced in the equilibrium equation by modifying the force density vector  $q$ .

Each element of  $q$  encodes the length ratio between form and force graph dual edges, the magnitude of forces may be controlled by the user by modifying specific elements of  $q$ . In the implementation, the elements of  $q$  are a functions of force magnitudes and interface drawing scale.

$$q_i = \frac{\text{force graph scale}}{\text{form graph scale}} * \frac{\text{force magnitude}}{\text{form graph edge length}}$$

Edges with force densities prescribed by user are referred to as *independent edges*. Modifying independent edges, different states of equilibrium may be explored for given structure. The independent edges are not an arbitrary selection, instead possible sets of independent edges are uniquely determined for each structure. Adding to the complexity, it is not obvious which sets are possible but instead some user experimentation may be necessary.

As self-stress is necessary for any solution but the arbitrary  $q = 0$ , prescription of independent edges is required. The required number of independent edges is equal to the system degree of static indeterminacy,  $k$ . In *Structural computations with the Singular value decomposition of the equilibrium matrix* (1993), author S. Pellegrino shows that the *rank-nullity theorem* can be applied to equilibrium matrix to find the degrees of static and kinematic (in)determinacy,  $k$  and  $m$ , according to 18 and 19 where  $r$  refers to the matrix *rank* of  $A$ .

$$(18) \quad k = n_c - r$$

$$(19) \quad m = n_r - r$$

The rank,  $r$ , is understood as the number of linearly dependent columns (or rows) of the equilibrium matrix  $A$ . Some columns are linear combinations of the other columns, these are said to be linearly dependent columns. Those that cannot be found to be a combination of the other columns are said to be linearly independent columns. Linearly dependent columns are also known as *pivots* and linearly independent as *non-pivot columns*. The rank of  $A$  is the number of pivots of  $A$

One way to find the rank of  $A$  is to rearrange it to its *row echelon form* (see below), the pivots are easily identified as columns containing the leading non-zero element in each row.

The values of  $k$  and  $m$  determine how the equilibrium equation should be solved and interpreted. For any solution to be available it is kinematic determinacy and static indeterminacy is required,  $m = 0$  and  $k > 0$ . The interpretation of  $k$  and  $m$  and its implications are further explored in *Algebraic graphic statics*.

### 3.6 Structural exploration

	<u>2954</u>	0	0	-3463	429	0	0
<i>rref(A)</i>	0	<u>2954</u>	0	0	-429	-1172	0
$[2v_i * e]$	0	0	<u>2954</u>	0	0	1172	-4926
	0	0	0	<u>6379</u>	-3750	0	0
	0	0	0	0	<u>3750</u>	-3750	0
	0	0	0	0	0	<u>3750</u>	-6662

By reduced row echelon form of  $A$  in studied case we find that the rank of  $A$  is six. Equation 18 informs that the degree of static indeterminacy is one and equation 19 inform that degree of kinematic indeterminacy is zero.

At this point the user is free to experiment with different sets of independent edges. In this case, since the static indeterminacy is one, one element of  $q$  must be prescribed. Not all variations of  $q$  will be a solution to the equilibrium equation. Which combinations that will produce a solution is unintuitive at best. A measure of user-experimentation is required to find a suitable variation of  $q$  to both satisfy the user exploration goals and equation solution.

A viable combination of independent edges in  $q$  can be found by studying the non-pivot columns of the reduced row form of matrix  $A$ . If it proves hard to identify a viable independent edge by experimentation, this may provide a viable but restricted solution. In this example we know from

studying the non-pivot columns of  $A$ , that a system with edge seven independent does solve for variable states of self-stress.

Form exploration with independent edges as variables is limited to exploration of force magnitude variations. Since the value of an independent edge translate to the magnitude of corresponding force, any variation in independent edge scale result in a corresponding shift in force graph magnitudes.

Given that the shape of a funicular is determined by the set of external loads it is exposed to, any variation of independent edge value will return a corresponding scale of force graph.

Different funiculars are found by geometrical construct. As such, the generation of different funiculars is a matter of front end GUI implementation. When a form is generated it is easily analysed for forces by exporting form node coordinates to back end algorithm.

The design force in edge one, two and three are known to be 13kN. In terms of self-stress this correspond to an equivalent force density of 4.4.

$$q_1 = \frac{\text{force graph scale}}{\text{form graph scale}} * \frac{13000}{\sqrt{u_1^2 + v_1^2}} = \frac{1}{1} * \frac{13000}{\sqrt{0^2 + 2954^2}} = 4.4$$

Solving the equilibrium equation with  $q_1$  prescribed to 4.4 results in  $q = [4.4; 4.38; 4.38; 4.76; 8.09; 8.09; 4.56]$  thus resulting in force graph coordinate difference vectors, force graph node coordinates and force graphs below;

$u^*$	0	$v^*$	13000	$X^*$	30330	$Y^*$	-16470
$[e \ x \ 1]$	0	$[e \ x \ 1]$	13000	$[v^* \ x \ 1]$	0	$[v^* \ x \ 1]$	-39000
	0		13000		0		-26000
	-30330		16470		0		-13000
	-30330		3470		0		0
	-30330		-9530				
	-30330		-22530				

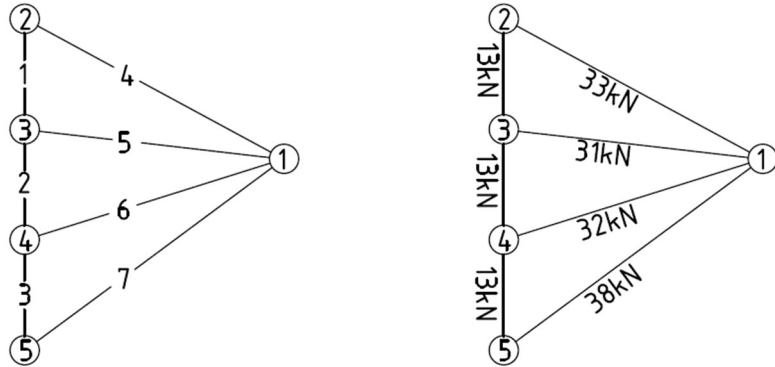


Figure 34. Resulting force graph from reciprocal transformation. Labelling (left) and magnitudes (right)

### 3.7 Discussion

A significant difference between computational and manual graphic statics method is the edges that are free to be used in exploration. The computational method is limited to a specific set of independent edges. The manual method on the other hand is not limited by any such technical requirements.

Using the manual method, one is free to modify both direction and magnitude of any edge. The only limitation is dictated by Bow's notation reciprocity. A change in either direction or magnitude will dictate a reciprocal change in another graph. Manual exploration in force graph may very well cause changes in form diagram.

The computational method is limited to downstream exploration from the form graph. In a full implementation the user is free to explore the effect of different forms by iterating different nodal positions or graph connectivity, but one is also limited the independent edges dictated by the equilibrium matrix.

The equilibrium matrix is generated from prescribed form graph and the equilibrium equation solved to produce the force graph. While this computational method produces quick calculations and accurate results it does not permit form graph to be generated from a prescribed force graph.

It is interesting to note that the algorithm is not simple invertible, as to produce a form graph from a prescribed force graph. In Blocks *Algebraic graphic statics* it is stated that such a backwards transformation is a matter of *constrained optimisation problem*. It is unknown to this author exactly why this is. One factor may be how the form graph has leaf nodes and the force graph does not. It may be that leaf nodes are necessary to achieve a state of self-stress in the system. An alternative viewpoint is that there may exist multiple form graphs to the same force graph. Any algorithm capable of transforming from force to form would thus have to handle selection between alternative solutions.

### 3.8 User interface

The reciprocity transformation algorithm may be implemented into a variety of user interfaces (UI). In this thesis, the mathematics software *GeoGebra* was tested for compatibility. A strategy for passing information between UI and back-end code should be presented and a proof of concept implementation illustrated.

Three factors make GeoGebra a suitable candidate as a user interface. First, it features a dynamic, easy to use yet powerful graph interface. Second, the software focus is on geometry and algebra and third, the software has an open source code and extensive scripting capabilities. With the back-end code running from a Python code IDE (integrated development environment) the integration challenge is a matter of Python code to GeoGebra communication.

For a fully integrated user experience, the UI needs to integrate simultaneous displays of both form and force graphs, the capability to draw and modify nodes and edges dynamically and to define independent edges. *GeoGebra* feature built in tools that potentially may be used in implementation for these purposes.

Primarily it is the graph- connectivity, topology and independent edges that should be passed between the Python code and GeoGebra. Form graph information should be passed from GeoGebra at drawing update to Python code; processed for reciprocal transformation and force graph information communicated back to GeoGebra. A possible strategy for passing information would utilize the Geogebra save file as a medium from which information can be read and written by both GeoGebra and Python code. This strategy should be examined in following section.

### 3.9 Proof of concept

The GeoGebra file format ‘.ggb’ is a zip-file containing three XML files, a thumbnail and a JavaScript file. The XML file named ‘geogebra.xml’ contains all information created in GeoGebra project files and the JavaScript file is initiated by GeoGebra at initiation of main program. These two files form the basis of this implementation strategy. A static communication system may be set up by reading and writing to- and -from the XML file whenever a form or force graph is updated.

```

<element type="point" label="B">
  <show object="true" label="false"/>
  <objColor r="0" g="0" b="255" alpha="0.0"/>
  <layer val="0"/>
  <labelMode val="0"/>
  <animation step="1" speed="1" type="1" playing="false"/>
  <coords x="-4.0" y="5.5" z="1.0"/>
  <pointSize val="5"/>
  <pointStyle val="0"/>
</element>
<command name="Segment">
  <input a0="A" a1="B"/>
  <output a0="f"/>
</command>
<element type="segment" label="f">
  <show object="true" label="false"/>
  <objColor r="0" g="0" b="0" alpha="0.0"/>
  <layer val="0"/>
  <labelMode val="0"/>
  <coords x="-2.0" y="1.5" z="-16.25"/>
  <lineStyle thickness="2" type="0" typeHidden="1"/>
  <outlyingIntersections val="false"/>
  <keepTypeOnTransform val="true"/>
</element>

```

Figure 35. Section of XML file contained in .ggb file.

Reading and writing .XML files is a task that Python is well suited for. Many code modules are available that makes the process easy by translating the XML format to an easy to read data-tree format. In the XML data tree a *constructions* branch contain all geometrical information created in GeoGebra. Relevant data may be extracted from the XML file by filtering for the sub-branch *elements* with type “point” and sub-branch *command* with name “Segment”. Writing the force graph- connectivity and topology to the XML file utilize the same code modules and follow the same procedure.

Using this method of passing information only a minimum of data interpretation is necessary. Only the indexing system requires a translation (from lettering system to vector element index) which is easy to achieve.

The form geometry is easily created in GeoGebra using the 'segment' tool. If desired it is possible to specify exact node positions using the algebra interface. The algebra interface is also useful to determine the form graph drawing scale. Figure 36 illustrates a form graph representing the suspension system carrying the bridge studied previously.

As the length of edges connected to leaf nodes are function of force densities, it is not necessary to specify exact magnitude of edges representing external forces. Instead the form graph length of independent edges is noted and compared to intended magnitude. In this case external force, 'edge j' should be prescribed to 13kN. The Algebra interface shows the length of 'j' as 1, thus the form graph scale is 1:13 [kN].

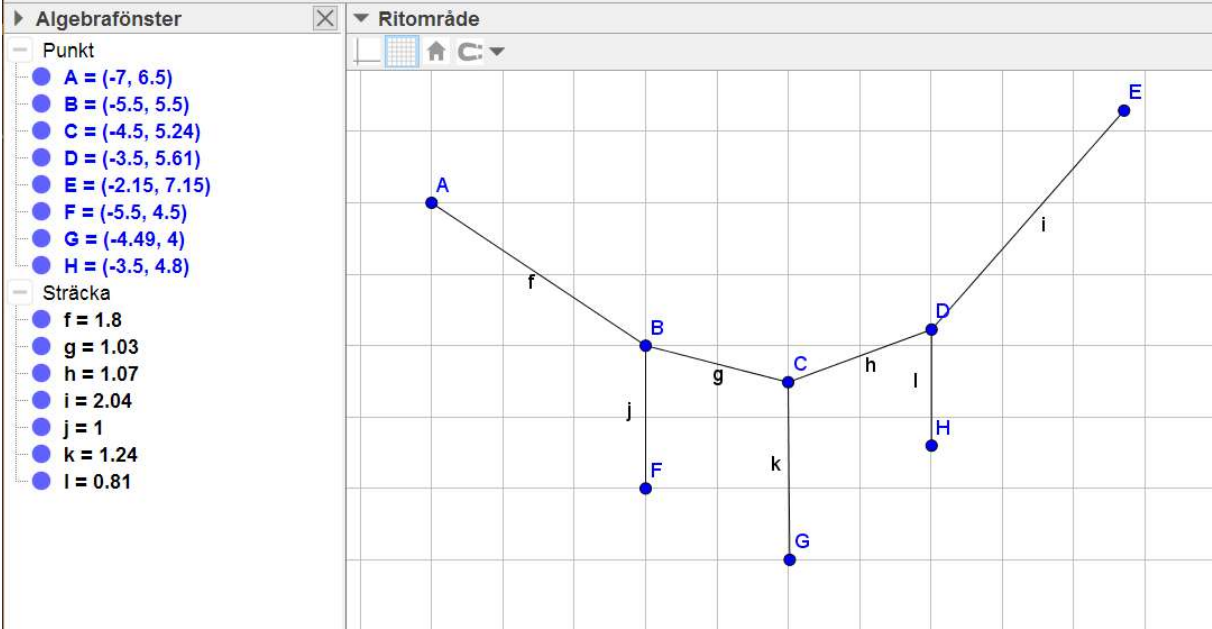


Figure 36. Approximate form geometry in GeoGebra

After saving the file, the geometry can be passed to Python using the presented XML method. Figure 37 illustrates the geometry as interpreted and indexed by Python code. As users are only concerned with the length and orientation of edges, only edges are labelled. We now know that we want to prescribe edge '4' as independent.

$q_4$  is here manually calculated after having Python print  $u$  and  $v$ . 1:1 force graph drawing scale is presumed.

$$q_4 = \frac{13}{1} * \frac{1}{\sqrt{0^2 + -1^2}} = 13 [N]$$

$u$	1.5	$v$	-1.0000
$[e \times 1]$	0.9978	$[e \times 1]$	-0.2563
	1.0049		0.3691
	1.3485		1.5331

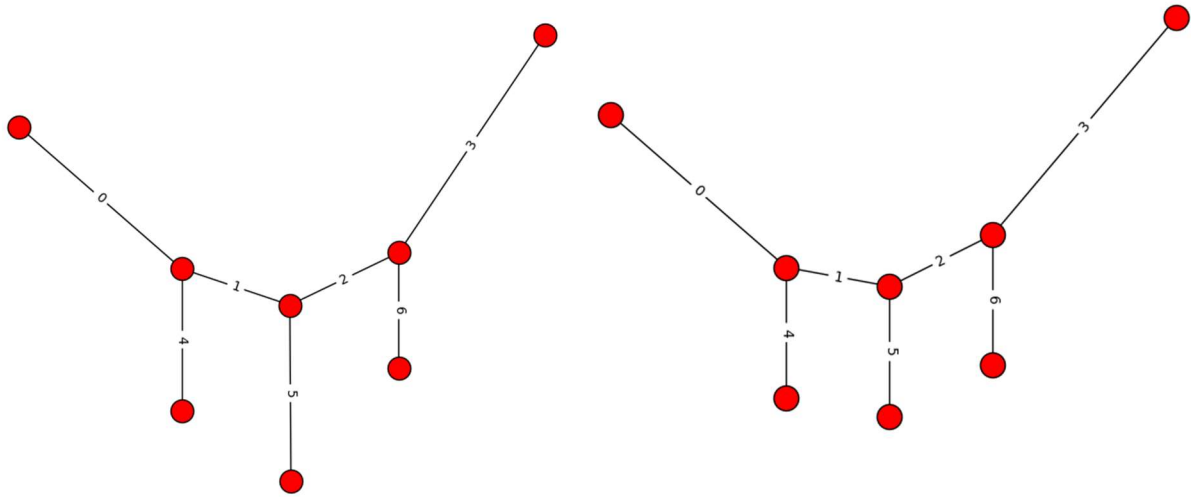


Figure 37. Left: GeoGebra approximate geometry. Right: Precise funicular geometry

The degrees of static and kinematic indeterminacy is calculated by an implementation following the algorithms proposed by Van Mele and Block in Algebraic graphic statics (2014). In this implementation, the user is presented with a Python console print out of degrees of indeterminacy, the reduced row echelon form of  $A$  and the prompt to select independent edge and prescribe force density. Resulting  $q$ ,  $x^*$  and  $y^*$  are calculated using presented back-end strategy, from which the force graph is generated. The results for illustrated case are presented below.

As the equilibrium equation was solvable given prescribed independent edge we know that the given geometry is funicular and in equilibrium. Notably this is not under the assumed load case of equal vertical forces (edge 4-6) but instead the geometry is funicular under different vertical forces (24kN, 19kN and 13kN).

```

System is 1 deg static- and 0 deg kinematic indeterminate
(Matrix([
[1.0, 0, 0, 0, 0, 0, -0.707807661700179],
[ 0, 1.0, 0, 0, 0, 0, -1.06300067905757],
[ 0, 0, 1.0, 0, 0, 0, -1.05101293426861],
[ 0, 0, 0, 1.0, 0, 0, -0.783260969211046],
[ 0, 0, 0, 0, 1.0, 0, -0.435302828930812],
[ 0, 0, 0, 0, 0, 1.0, -0.531116666936273]]), [0, 1, 2, 3, 4, 5])
Choose 1 independent edge(s).

```

```

Select independent edges: [4]
Select force densities: [13]
force densities are:
[ 21.13815714  31.74573632  31.38773111  23.39151488  13.          15.86141006
 29.86426721]

```

Figure 38. Python console print out prompting selection of independent edge(s).

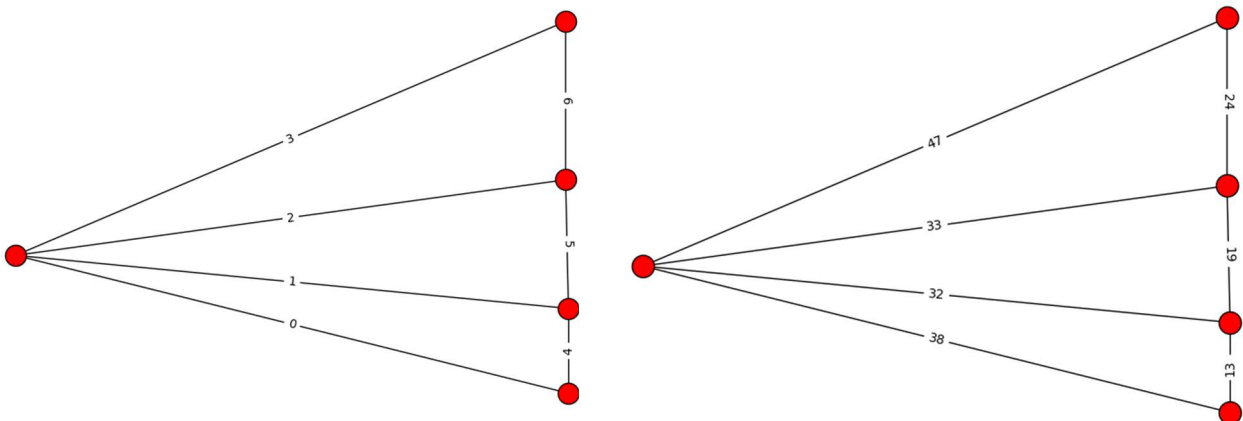


Figure 39. Resulting force graph from approximate geometry. Labeling (left) and magnitudes (right).

### 3.10 Discussion

Using the proposed XML method, geometric information may be passed between GeoGebra and python. The 'static' information exchange is successfully implemented. The form graph geometric data may be passed from GeoGebra interface to Python. The XML strategy also works well for passing geometric data from Python to GeoGebra. This method is easy to implement and only limited measures are required to translate between data formats.

The XML method strategy incorrectly supposed that any geometry update would automatically update the XML file, instead GeoGebra utilizes a system of temporary files embedded with the source code. The proposed method requires the user to actively save GeoGebra file to pass geometric data for reciprocity transformation. The data passed from Python to XML file cannot be automatically updated in runtime. The user is required to restart GeoGebra for graph update. A 'dynamic' data exchange is not achieved with proposed XML method.

An automatic graph update from XML file could potentially be solved by incorporating GeoGebra script observer classes through Java script. The JavaScript file contained within the .ggb file is automatically initiated when .ggb file is loaded. Native GeoGebra script methods are available through the JavaScript. Incorporating the GeoGebra observer classes this way, it may be possible to manage UI redraws and automatically initiate force graph recalculations.

The results from the presented transformation illustrate a significant flaw in the proposed user interface implementation. As funiculars are very form sensitive, accurate calculations require accurate funicular geometry. Using the proposed point-and-click interface with GeoGebra, geometry is easily generated and visually accurate. The form graphs illustrated in figure 37 are visually indistinguishable (besides length of external forces). Figure 'a' is the geometry generated using GeoGebra interface and 'b' the exact funicular form generated using Wolfe's methods. At worst, this approximation corresponds to a force magnitude error of 40%.

This error may be circumvented in the current implementation by utilizing the large Geometry toolbox available in GeoGebra. Wolf's method of generating funiculars may be used to create the specific form required for a specific load case. From this geometry, the presented back-end strategy is very capable of accurate transformation to force graph.

The result also demonstrates a significant difference to the traditional methods. In the manual methods, external forces are defined in the force line and a suitable form found to satisfy equilibrium. Or alternatively, from a proposed form an external load case may be found that satisfy equilibrium.

The automatic method does not differentiate so clearly between form- or force- exploration. In each iteration of the transformation calculation independent edges are determined from input form geometry. The user has only a limited say in what independent edge to use. External and internal forces are the same to the equilibrium equation. It may be that the independent edges are either force- or form- edges or both.

This complexity is illustrated by the resulting magnitudes of the presented transformation. The approximate geometry failed to accurately represent the funicular geometry for the intended load case, the transformation algorithm calculated a load case for which the structure is funicular.

## 4. CONCLUSION

Initially developed as a practical method for structural analysis and design, and later effectively antiquated in the computational age; graphic statics is making a come-back in the context of structural exploration.

As demonstrated in first part of this thesis, traditional graphic statics methods are still viable as a means of understanding and exploring structures. The graph interface and the simultaneous interaction with form and forces offer a great interface to explore structures. The simplistic nature of the graphic statics requires the user to understand the disparity between model and reality. The simplistic model should as such encourage the user to create form that utilise the material in line with their properties.

The second part of this thesis has illustrated two pioneering developments in structural exploration. The examples show that cross discipline topology design is key to creating new form. By integrating analysis and design it is possible to identify new structural form that fulfil a broad spectra of design criteria.

The third part of this thesis has illustrated a strategy for representing graphs and graph reciprocity in software. The strategy does successfully represent reciprocal graphs but in a significantly different way than traditional graphic statics. The computational strategy is limited by how many and what combinations the user can prescribe to magnitude of.

Graphic statics features some interesting methods that unfortunately will have limited use in practice. The simplistic model is both its strength and its greatest weakness. The simplicity allows greater interactivity and encourages designs in line with material properties. Yet the model is only applicable to a very limited set of structures (mainly pin jointed structures and thin vaults). Other types of structures may be modelled in analogy with a graphic statics model but for the most common types of building structures it is not applicable.

It was suggested that Graphic statics might contribute to *material sustainability, architectural developments based in honest design and reduced projection costs*. While it certainly has the appropriate features for such a contribution; considering the niche applications, the total contribution is marginal. Graphic statics is perhaps most relevant as an educational tool teaching important aspects of structural engineering.

As an educational tool, Graphic statics methods serve to highlight the possibilities available in the topology and shape analysis to reduce material consumption and achieve greater performance. Teaching graphic statics methods serves to integrate analysis and design.

It is the view of this thesis author it is fundamental to understand model assumptions and presumptions. Considering the model-reality is an essential process to develop knowledge. Working with the Graphic statics model is an excellent educational process to reflect on the model-reality disparity. The simplistic nature of the model forces the user to think outside of the calculation process and consider model assumptions.

In conclusion; besides some niche applications in practice, the greatest benefit of Graphic statics is as an educational tool teaching model consideration and benefits of structural exploration. By developing the engineering mindset, Graphic statics may indirectly contribute to *material sustainability, architectural developments based in honest design and reduced projection costs.*

## 5. REFERENCES

- Allen, Edward., Zalewski, Waclaw. 2010. *Form and forces; designing efficient, expressive structures*. Hoboken, New Jersey: John Wiley & Sons.
- Baker, William F., Beghini, Lauren L., Mazurek, Arkadiusz., Carrion, Juan., Beghini, Alessandro. 2013. Maxwell's reciprocal diagrams and discrete Michell frames. *Structural and multidisciplinary optimization* 48: 267-277.
- Baker, William F. 2015/12/1. *On the harmony of theory and practice in the design of tall buildings*. H.C Ørsted Lecture, DTU.  
[https://www.youtube.com/watch?v=\\_XrvfBlcWcs](https://www.youtube.com/watch?v=_XrvfBlcWcs) (Link valid 2017-04-22)
- Beghini, L Lauren., Behini, Alessandro., Katz, Neil., Baker, William F., Paulino, Glaucio H. 2014. Connecting architecture and engineering through structural topology optimization. *Engineering structures* 59: 716-726.
- Beghini, Lauren L., Carrion, Juan., Beghini, Alessandro., Mazurek, Arkadiusz., Baker, William F. 2013. Structural optimization using graphic statics. *Structural and multidisciplinary optimization* 49: 351-366.
- Block, Philippe. 2005. *Equilibrium systems Studies in Masonry Structure*. M.Sc., Massachusetts Institute of Technology.
- Block, Philippe., DeJong, Matt., Ochsendorf, John. 2006. As hangs the flexible line: Equilibrium of masonry arches. *Nexus network journal* 8: 9-19.
- Clune, Rory., Connor, Jerome J., Ochsendorf, John A., Kelliher, Denis. 2012. An object-oriented architecture for extensible structural design software. *Computers and structures* 100-101: 1-17.
- Fivet, Corentin., Zastavni, Denis. 2014. A fully geometric approach for interactive constraint-based structural equilibrium design. *Computer-aided design* 61: 42-57.
- Heyman, J. 1995. *The stone skeleton: Structural engineering of masonry architecture*. Cambridge UK: Cambridge university press.
- Melbourne W. H. 1995 The response of large roofs to wind action. *Journal of wind engineering and industrial aerodynamics* 54-55: 325-335
- Micheletti, Andrea. 2008. On generalized reciprocal diagrams for self-stressed frameworks. *Int. J. Space structures*
- Moseley, Henry. 1843. *The mechanical principles of engineering and architecture*. London: Longman, Brown, Green and Longmans.
- Mueller, Caitlin T., Ochsendorf, John A. 2015. Combining structural performance and designer preferences in evolutionary design space exploration. *Automation in Construction* 52: 70-82

Mueller, Caitlin., Ochsendorf, John. From analysis to design: a new computational strategy for structural creativity. *Proceedings of the 2<sup>nd</sup> international workshop on design in civil and environmental engineering*: 46-56.

Pajnowska, Karolina. 2016. *Embedded time-scapes*.

<https://www.behance.net/gallery/38176539/Embedded-time-scapes> (Link valid 2017-04-22)

Pedreschi, R., Theodossopoulos, D. 2007. The double-curved masonry vaults of Eladio Dieste. *Proceedings of the ICE – Structures and Buildings* 160: 3-11.

Pellegrino, S. 1993. Structural computations with the singular value decompositions of the equilibrium matrix. *Int. J. Solid Structures* 30: 3025-3035.

Rahal, Khaldoun. 2008. Simplified design and capacity calculation of shear strength in reinforced concrete membrane elements. *Engineering Structures* 30: 2782-2791.

Van Mele, Tom., Block, Philippe. 2014. Algebraic graph statics. *Computer-aided design* 53: 104-116.

Van Mele, Tom., Lachauer, Lorenz., Rippmann, Matthias., Block, Philippe. 2012. Geometry based understanding of structures. *J. IASS*: 285-295

Wolf, William S. 1921. *Graphical analysis a textbook on graphic statics*. New York: McGraw-hill book company inc.